PETRO-GEOCHEMICAL INVESTIGATION OF THYOLO MOUNTAIN PERTHITIC SYENITES AND PERTHITE GNEISS

Bryan Chabuka

(Esc/004/20)

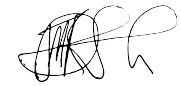
Thyolo, Malawi

The dissertation was submitted to the Ndata School of Climate and Earth Sciences of the Malawi University of Science and Technology in partial fulfillment of the requirements for a Bachelor of Science Degree in Earth Sciences.

Date: 29th April, 2025

Dissertation approved by:

Supervisor:

Mr. M. Mtonda Signature: 

Assessor: signature:

Title, Initials, Name Signature:

I, Bryan Chabuka, declare that the work in this dissertation titled “Petro-Geochemical Investigation of Thyolo Mountain Perthitic Syenites and Perthite Gneiss” has been carried out by me. All information retrieved from other literature has been acknowledged in the text, and a list of references has been provided.

Disclaimer

This document describes work undertaken as part of a study at the Ndata School of Climate and Earth Sciences of the Malawi University of Science and Technology. All views and opinions expressed therein remain the sole responsibility of the author(s) and do not necessarily represent those of the school.

COPYRIGHT STATEMENT:

This dissertation copy has been supplied on the condition that anyone who consults it is understood to recognize that its copyright rests with its author and that no quotation from the dissertation and no information derived from it may be published without acknowledgement.

Abstract

This study investigates the geochemical characteristics of perthitic syenites and perthite gneiss from the Thyolo mountain in southern Malawi to understand petrogenesis and geological history. Field observations, petrographic analysis, geochemical data, and statistical methods were used to characterize these rocks. The key findings indicate that the perthitic syenites are predominantly pink or brownish, dark gray, and whitish with phaneritic textures showing high K2O and Na2O values typical of alkaline nature. Most samples are metaluminous, consistent with rift or post-orogenic magmatism. Granite characterized by high SiO2 values and slightly peraluminous nature, likely representing a late-stage differentiate or separate intrusive phase. Perthite gneisses are dark grey, coarse-grained, dominated by dark mineral grains like hornblende and pyroxene, showing mafic compositions distinct from syenites due to their trace element signatures. The petrogenesis of perthitic syenites suggests derivation from silica-oversaturated alkali-rich magma, indicative of extensional settings possibly related to the East African Rift System (EARS) or post-orogenic events after the Pan-African orogeny—perthitic textures formed during slow cooling typical of deep-seated crustal environments. The granite's high SiO2 values suggest derivation from partial melting of crustal material, potentially representing a differentiated fraction of the syenitic magma. Perthite gneisses likely represent metamorphosed igneous protolith under amphibolite and granulite facies conditions, with deformation textures indicating tectonic forces linked to either Pan-African orogeny or rifting. The alkaline shoshonitic nature of the syenites suggests formation in an extensional or post-orogenic setting linked to Neoproterozoic magmatism or Mesozoic rifting associated with the Chilwa alkaline province (CAP). Gneisses reflect high-grade metamorphism within the Mozambique belt during the Pan-African orogeny, with deformation features aligning with EARS-related faulting. These rocks have economic potential: perthitic syenites are suitable for ceramics, glass, and construction applications due to high feldspar content with elevated Ba and Sr, suggesting potential for barite or strontiate deposits. Perthite gneisses are suitable for construction aggregates, road base, or ornamental stone. Granitic rocks are useful in ceramics or dimension stone.

Acknowledgements

I would like to thank my parents, Mr. and Mrs. Chabuka, who sponsored this work and who have been the pillar of my life for as long as I have lived on earth.

Special thanks go to my siblings, Reconcile, Honest, Respect, and Eliazer, and not forgetting my elder brother, Stuart, all of whom have always been there for me throughout my entire life and have supported me.

I would like to thank my supervisor, Mr. M. Mtonda, for his guidance and encouragement during this research.

I would like to thank all my friends and family who make my life a paradise

Dedicated to my Parents, Mr. and Mrs Chabuka.

Table of Contents

Chapter 1 Introduction 11

1.1. Background 14

1.2. Problem statement 15

1.3. Main and Specific Objectives 15

1.3.1. Specific objectives 16

Chapter 2 Literature Review 17

2.1. General geology of Malawi 17

2.2. The East African Rift System and Its Influence on Malawi's Geology 20

2.3. Geology of Thyolo 21

2.4. Syenitic and Gneissic Rocks: definitions and characteristics 22

2.4.1 Syenites 22

2.4.2. Gneiss 23

2.5. Perthite 24

2.6. Regional occurrences of perthitic syenites and perthite gneiss 24

2.6.1. World 24

2.6.2. Africa 25

2.6.3. Malawi 26

2.7. Geochemical studies on syenitic and gneissic rocks 26

2.7.1. World 26

2.7.2. Africa 28

2.7.3. Malawi 28

2.8. Metamorphism and magmatic differentiation of syenitic and gneissic rocks 28

2.8.1. Magmatic Differentiation of syenitic rocks 28

2.8.2. Magma source and tectonic setting 29

2.8.3. Metamorphism of Gneissic rocks 29

2.8.4. Metamorphic processes 30
2.8.5. Perthite in Gneisses 30
2.8.6. Tectonic setting 30
2.9. Economic and industrial significance of perthitic syenites and perthite gneiss 30
2.10. Knowledge gaps and justification for the study 33
2.10.1. Petrogenesis 33
2.10.2. Economic rationale 34
2.10.3. Environmental impact 34
Chapter 3 Methodology 35
3.1. Research design 35
3.2. Geological Survey 35
3.3. Sampling and Analysis 38
Chapter 4 Results and Discussions 46
4.1. Geochemistry 46
4.2. Alumina Saturation Indices (ASI) 56
4.3. Petrographic Analysis 57
4.4. Statistical Analysis 59
4.4.1. Principal Component Analysis 59
4.4.2. Cluster Analysis 60
4.5. Discussions 62
4.5.1. Characterization and Classification 62
4.5.2. Petrogenesis 63
4.5.3. Tectonic evolution 65
4.5.4. Economic and industrial significance 66
4.5.5. Environmental implications 66
Chapter 5 Conclusion and Recommendations 67

5.1. Conclusion 67
5.2. Recommendations 68
Chapter 6 References 70

List of Figures

- Figure 1: Map showing the regional geology of Malawi as suggested by Karmakar & Schenk (2016), indicating Mesoproterozoic orogenic rocks (Huang, 2017).
- Figure 2: Geological map of Malawi based on Smedley and Kinniburgh (2013) (Rivett et al., 2018).
- Figure 3: Map showing the locations of mobile belts in the East African region, with Malawi indicated in the red box (modified after Ring et al., 1997). Dark blue areas represent the Indian Ocean, and light blue areas represent African lakes (Huang, 2017).
- Figure 4: Syenite rock.
- Figure 5: Gneiss rock.
- Figure 6: Nepheline syenite ceramic flour (Bhoomi Pottery, https://www.bhoomipottery.com/products/laguna-clay-nepheline-syenite-a-270-india). [Page]
- Figure 7: Gneiss wall decoration.
- Figure 8: Rainbow lattice sunstone.
- Figure 9: Tools used during the survey.
- Figure 10: Sampling point map of Thyolo Mountain.
- Figure 11: Total Alkali-Silica (TAS) diagram for samples from Thyolo Mountain.
- Figure 12: Major element versus SiO_2 plots for samples from Thyolo Mountain.
- Figure 13: Primitive mantle-normalized spider diagram for samples from Thyolo Mountain.
- Figure 14: Chondrite-normalized Rare Earth Element (REE) spider diagram for samples from Thyolo Mountain compared to rare element spider diagram.
- Figure 15: Peraluminosity classification plot for samples from Thyolo Mountain.
- Figure 16: Microphotographs of Thyolo Mountain samples.
- Figure 17: Principal Component Analysis (PCA) biplot of samples from Thyolo Mountain.
- Figure 18: K-means clustering in Principal Component Analysis space of samples from Thyolo Mountain.
- Figure 19: Silhouette plot for K-means clustering of samples from Thyolo Mountain.

List of Tables

- Table 1: Data collected during the survey, including sampling locations, sample IDs, GPS coordinates, elevation, and outcrop descriptions from Thyolo Mountain.
- Table 2: X-ray Fluorescence (XRF) data for major, minor, trace, and rare earth elements of rock samples from Thyolo Mountain, analyzed at the Geological Survey in Zomba.
- Table 3: Normalized major oxides of samples from Thyolo Mountain, showing compositions such as SiO_2, Na_2O, and K_2O.
- Table 4: Primitive Mantle-Normalized Trace Element Concentrations (ppm) for rock samples from Thyolo Mountain, including Rb, Sr, and Ba.
- Table 5: Chondrite-Normalized Rare Earth Element (REE) Concentrations (ppm) for rock samples from Thyolo Mountain, including La, Ce, and Nd.
- Table 6: Alumina saturation indices and classification for Thyolo Mountain samples, indicating metaluminous or slightly peraluminous compositions.

List of Abbreviations

- A/CNK: Molar ratio of $Al_2O_3/(CaO + Na_2O + K_2O)$
- A/NK: Molar ratio of $Al_2O_3/(Na_2O + K_2O)$
- ASI: Alumina Saturation Index
- Ba: Barium
- CAP: Chilwa Alkaline Province
- EARS: East African Rift System
- Fe_2O_3: Iron(III) Oxide
- GSD: Geological Survey Department
- HFSE: High Field Strength Elements
- K_2O: Potassium Oxide
- LILE: Large Ion Lithophile Elements
- MgO: Magnesium Oxide
- MUST: Malawi University of Science and Technology
- Na_2O: Sodium Oxide
- PCA: Principal Component Analysis
- ppm: Parts Per Million
- REE: Rare Earth Elements
- SiO_2: Silicon Dioxide
- Sr: Strontium
- TAS: Total Alkali-Silica
- UNIMA: University of Malawi
- wt.%: Weight Percent
- XRF: X-ray Fluorescence

Chapter 1 Introduction

1.1. Background

Malawi sits in east-central Africa, bordered by Tanzania, Mozambique, and Zambia, covering 118,484 km^2, 94,080 km^2 is land (Carter & Bennett, 1973). Its geology is complex simply because it is at the intersection of three ancient orogenic belts, the Ubendian (1.0 Ga – 540 Ma), Irumide (1.0 Ga – 500 Ma), and Mozambique belts (Neoproterozoic to early Cambrian). These were affected and reactivated by numerous tectonic events, including the Ubendian, Kibaran, Irumide, and Pan-African orogenies, leaving a scarred crust that is now splitting again with the East African Rift's southern end (Huang, 2017; Malunga, 2018). Most of Malawi is underlain by the Malawi basement complex, a bunch of Precambrian to early Paleozoic crystalline rocks old, beat, and complex (Carter & Bennett, 1973). The geology of Malawi follows a distinctive stratigraphic sequence. It starts with the basement complex. Unconformably overlying the complex is the Karoo super group, a collection of Permian-Carboniferous to lower Jurassic sedimentary and subordinate volcanic rocks found north and south of the country (Carter & Bennett, 1973; Jacobs et al, 2005). Next is the Chilwa Alkaline Province, consisting of intrusive rocks south of the Jurassic-Cretaceous (Carter & Bennett, 1973). Finally, Superficial deposits cover Lake Malawi's shore, Shire Valley, and the plains of Lilongwe and Mzimba (Carter & Bennett, 1973).

Thyolo is located in the southern region of Malawi and occupies 2600 km2, bordered by Blantyre, Chiradzulu, Mulanje, Chikwawa, and Nsanje. It has rugged terrain where elevations range from 53 m at Chiromo to 1,462 m at the peak of Thyolo Mountain. Three physiographic zones define the area: Shire Valley Plain, Thyolo Fault, Scarp Zone, forming the eastern boundary of the southern section of the Malawi Rift Valley, and the Thyolo highlands (Habgood et al., 1973). Thyolo mountain shines for its extensive syenitic rocks, big coarse-grained rocks filled with microperthite, oligoclase, and hornblende, low on quartz, grading into migmatites and gneisses (Habgood et al., 1973). The syenite likely formed through regional migmatization, corresponding to the basement's long, harsh history (Habgood et al., 1973).

Malawi's geology lacks modern high-resolution studies. Some knowledge on Malawi's geology is based on old geological maps, a lack of metamorphic studies, limited

petrological and geochronological data (Chisambi et al., 2022; Huang, 2017). The series of orogenies that affected the country's geology make deciphering information about the country's geology difficult (Tsunogae et al., 2021). Thyolo Mountain was studied by Habgood et al. (1973), syenites and gneisses, focusing on mapping the area and mineralogy, but poor emphasis was put on petrogenesis. Due to its critical location at the epicenter of three orogenies, it is important to understand the geology of Malawi to solve various supercontinental reconstructions and collision events related to the assembly of Gondwana (Huang, 2017; Tsunogae et al., 2021). Thyolo Mountain is important for its role in understanding regional tectonic, magmatic processes and resource potential.

1.2. Problem statement

Perthitic syenite and perthite gneiss occur in various geological settings worldwide, and understanding their distinct geochemistry and petrography can be used to decipher their petrogenesis. Perthite gneiss is often linked to high-temperature and pressure conditions, and perthitic syenites hint at complex geological processes like migmatization, magmatic differentiation, and metamorphism. Thyolo Mountain has both, and here lies an opportunity to study this formation at a high resolution, therefore providing a foundation for more modern studies. This study has the potential to elucidate Thyolo Mountain's role in the geology of the region, Malawi's rift or basement evolution, and to identify industrial potential, such as perthites used in ceramics, glass, and sometimes gems. This study also has the potential to provide quantitative data on geochemistry and petrography, which will help with the accuracy of knowledge of the formation. This study aims to achieve this through XRF data and petrography to elucidate the formation and geological evolution, and the significance of Thyolo Mountain in the region.

1.3. Main and Specific Objectives

This study aims to investigate the geochemical characteristics and petrography of perthitic syenites and perthite gneiss from the Thyolo mountain to figure out their petrogenesis and history.

1.3.1. Specific objectives

To determine the major element composition of perthitic syenites and perthite gneiss using geochemical analysis

To determine the trace element composition of perthitic syenites and perthite gneiss using geochemical analysis

To characterize the mineral assemblages and textural features of perthitic syenites and perthite gneiss using petrographic analysis

Chapter 2 Literature Review

2.1. General geology of Malawi

Most of Malawi is made up of Precambrian to early Paleozoic crystalline rocks called the basement complex (Carter & Bennett, 1977). The basement complex is dominated by medium to high-grade metamorphic rocks (Carter & Bennett, 1977). Rocks of the basement complex are semi-pelitic biotite gneiss with intercalated felsic to intermediate orthogneisses, metabasites, and metasediments (Tsunogae et al., 2021). North and south of the country, the basement complex is uncomformably covered by sedimentary and subordinate volcanic rocks of permo Triassic to quaternary age intruded by basaltic or dolerite dykes and sills called the Karoo sedimentary rocks (Carter & Bennett, 1977). , Chilwa alkaline province, occur widely throughout southern Malawi and are intrusions of syeno-granitic and nepheline syenite rocks that were later intruded by volcanic rocks infilled by carbonatite and alkaline dykes of late Jurassic to early Cretaceous age (Jacobs et al., 2005). The cretaceous chilwa alkaline province (CAP) contains granites, syenites, nepheline syenites, basanites, phonolite dykes and minor carbonatite bodies (Carter & Bennett 1977). It is a series of late Cretaceous alkaline and carbonatitic intrusive and extrusive rocks exposed over about 64,00km^2 (Lewis et al., 2016). The province includes the first carbonatites to be recognized in Africa (Lewis et al., 2016). Various volcanics are found in the CAP in areas such as the Nakumba peninsula, Songwe Hill, and Michenga. They formed in response to extensional tectonics and mantle upwelling preceding the full development of the East African Rift System (Carter & Bennett, 1977). Superficial deposits cover a large region of Malawi's coastal area, the Shire Valley, and

the Lilongwe, Kasungu, and Mzimba plains (Carter & Bennett, 1973).

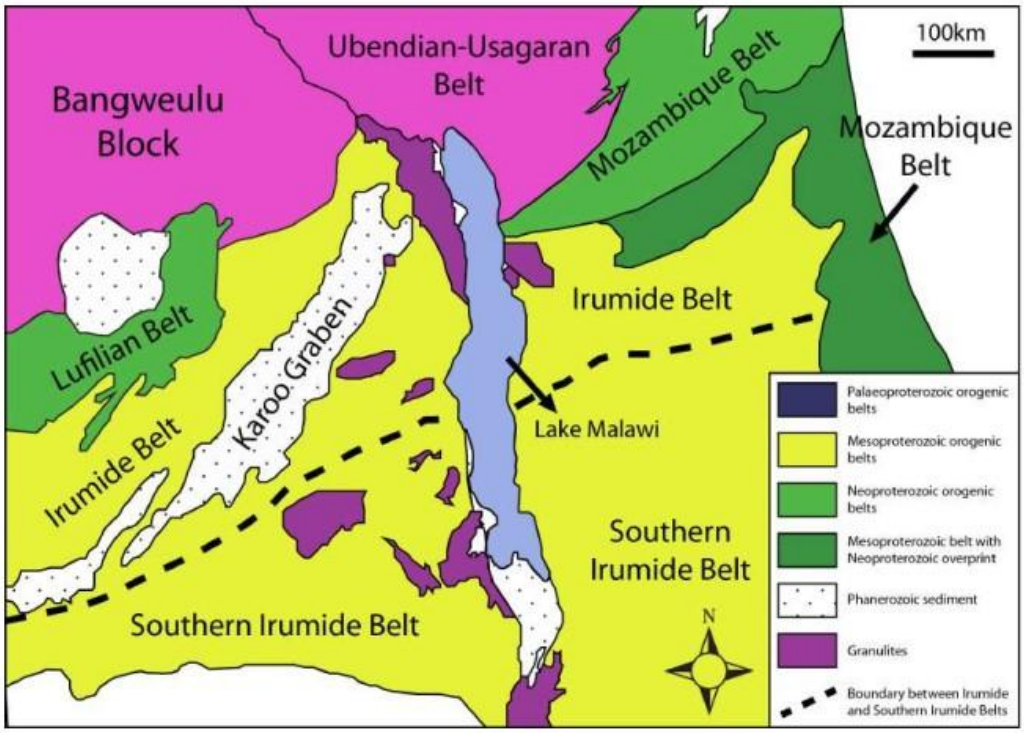


Figure 1: Map showing the regional geology of Malawi as suggested by Karmakar & Schenk (2016), which shows that Malawi consists of Mesoproterozoic orogenic rocks (Huang, 2017).

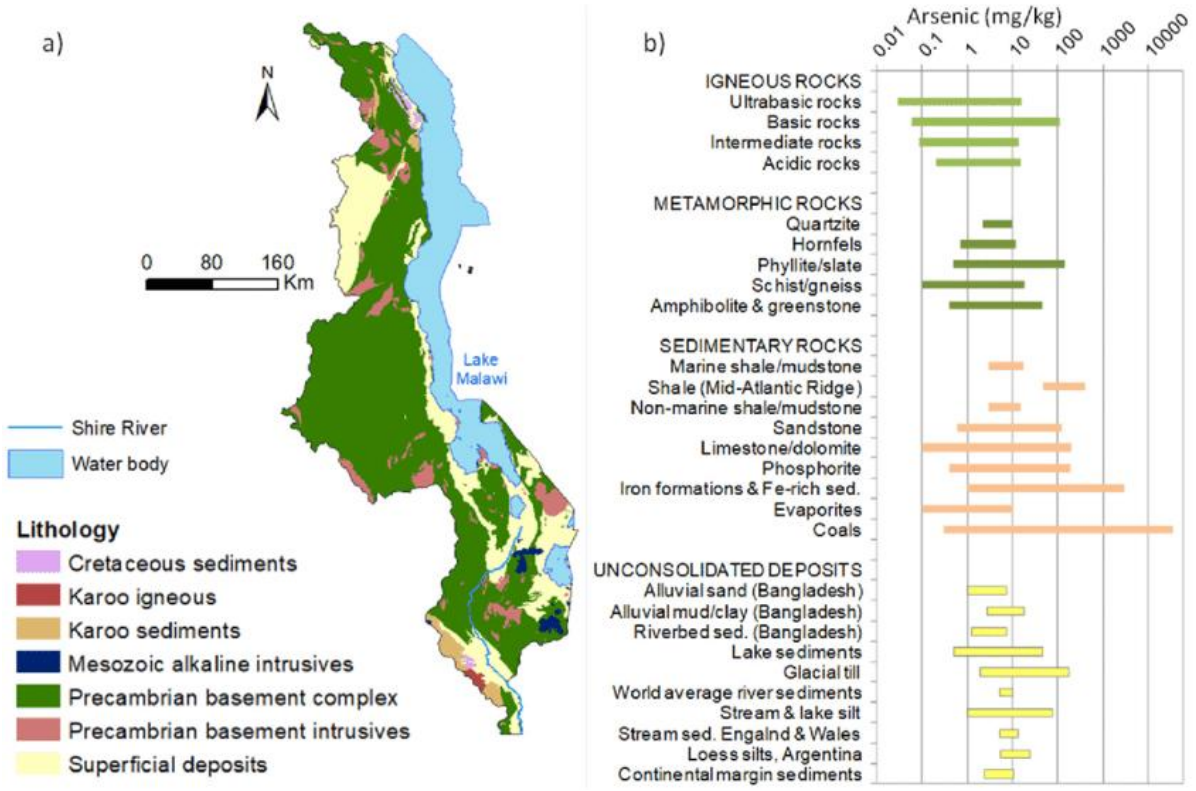


Figure 2: Geological map of Malawi based on Smedley and Kinniburgh (2013) (Rivett et al., 2018)

Malawi was affected by several tectonic events such as Rodinia assembly, Ubendian, Irumide, Kibaran, and pan African orogenies. (Manda et al., 2018; Huang, 2017). This complexity makes identifying features of older orogenic events that have already experienced multiple metamorphic overprinting from subsequent events difficult (Huang, 2017). Malawi lies at a key point in the zone of intersection between two fundamental suture zones associated with Gondwana assembly, the East African and Kuunga orogens (Manda et al., 2018). Malawi is still tectonically active as the southern end of the East African Rift System (Huang, 2017). The Southern Malawi basement complex is considered part of the Mozambique belt, made by a series of collisions between Archean cratons and/or Proterozoic magmatic arcs during Neoproterozoic to Cambrian time (Tsunogae et al., 2021). The region is important because of its location near the junction between East African and Kuunga orogens, meaning that complex magmatic and metamorphic episodes may have been recorded in high-grade metamorphic rocks in the region (Tsunogae et al., 2021).

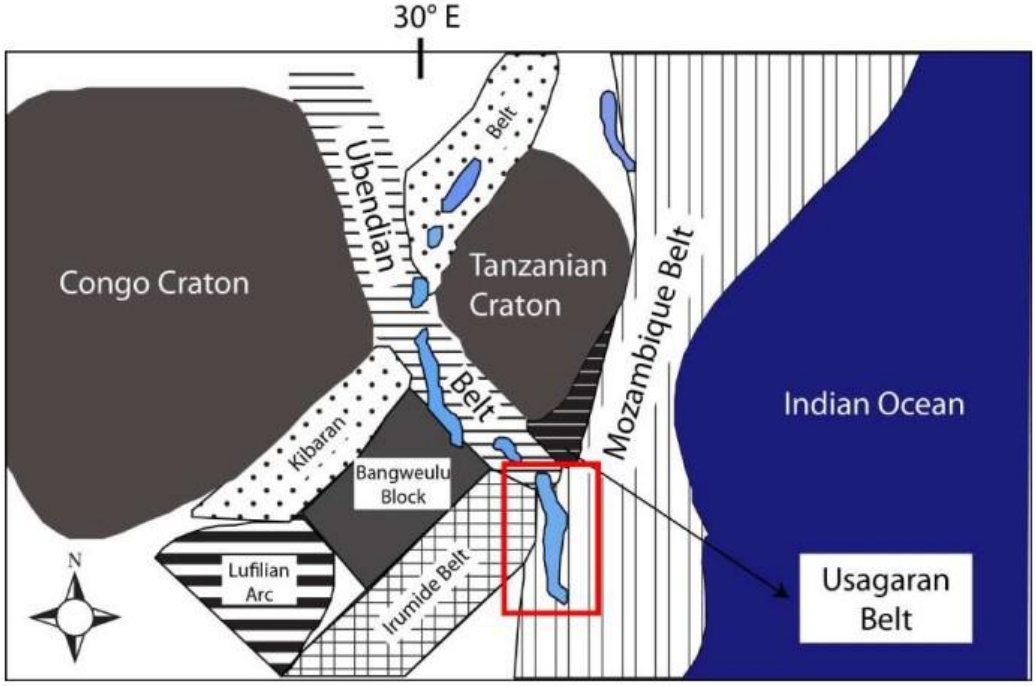


Figure 3: Map showing the locations of mobile belts in the East African region, where the location of Malawi is indicated in the red box (modified after Ring et al., 1997). The area shaded in dark blue represents the Indian Ocean, while areas shaded in light blue represent African lakes (Huang, 2017).

2.2. The East African Rift System and Its Influence on Malawi's Geology

The East African Rift System is the best example of an active rift in the world, although its origins are poorly understood (Macgregor, 2015). It is an intracontinental ridge system consisting of an important rift (Chorowicz, 2005). The most distinguishing features in it are narrow elongated zones of thinned continental crust shown on the surface by thermal uplift of the rift shoulders, the graben valleys and basins, and a major border fault in the crust linked to a low-angle detachment fault (Chorowicz, 2005). It is driven by the extension and thinning of the African plate (Scoon, 1958). Rifting started during the Oligocene and has continued through the Miocene, Pliocene, Pleistocene, and into the Holocene (Scoon, 1958). It is the largest volcanic province on Earth. It is divided into two branches: the eastern branch, which is older and more volcanically active, and the western branch is younger and less volcanic (Ring, 2013; Scoon, 1958). Rifting involves three stages: pre-rift, half-graben, and full graben. Rifting has had a

prominent effect on the geomorphology of East Africa, including drainage patterns, including major rivers like the Nile (Scoon, 1958).

The Malawi Rift is a southern extension of the western branch of the East African rift system (Chapola & Kaphwiyo, 1992; Ring, 1994). It is mainly occupied by Lake Malawi and consists of a series of half-grabens. It is at an early stage of development and is still seismically active, with much of the activity being associated with rift faults (Chapola & Kaphwiyo, 1992; Chorowicz, 2005). Rift faults recharged crustal structures whenever they were properly aligned with the extension directions (Ring, 1994). The lower Shire Valley in south Malawi is partly reworked by the East African rift system (Castaing, 1990). Thyolo fault bounds the north-eastern edge of the Shire Graben, located at the southern end of the largely amagmatic branch of the East African Rift, and has a current geodetic extension rate of ~2mm/ year (Wedmore et al., 2020). With the Thyolo fault scarp present in the area, what implications does it have on the Thyolo mountain formation and evolution

2.3. Geology of Thyolo

High-grade predominantly migmatic gneisses and granulites belonging to the basement complex carry much of the area and make up part of the extensive Precambrian to lower Paleozoic Mozambique belt (Habgood et al., 1973). The Thyolo basement complex is dominated by biotite hornblende gneisses and charnockitic granulites. It has experienced regional metamorphism under amphibolite to granulite facies conditions, which was followed by widespread migmatization and later syenitization, which is believed to be responsible for the formation of the Thyolo mountain syenite (Habgood et al., 1973). Chilwa alkaline province alkaline dyke rocks were intruded during the late Jurassic and early cretaceous and stand out in the northeast and are believed to be associated with the intrusion of the Mulanje syenite (Garson & Walshaw, 1969). Superficial deposits cover metamorphic and igneous rocks, mainly in the northeast (Habgood et al., 1973). No sufficient deposits of economic importance have been observed, although certain ultramafic bodies yield high base metal values, and a small section of copper has been reported at Ngala Hill (Habgood et al. 1973)

2.4. Syenitic and Gneissic Rocks: definitions and characteristics

2.4.1 Syenites

The name syenite was first used by Pliny the Elder (AD 23/24-79), a Roman author, naturalist, and naval and army commander. Syenite is a coarse-grained igneous rock of the same general composition as granite but with quartz either absent or present in a relatively small amount (Hall, 1987). Syenites are hololeucocratic to leucocratic intermediate and rarely mesocratic igneous rocks formed from cooling of a crustal or mantle silica saturated to silica under saturated magma (Kanouo et al., 2019). The feldspar component of the syenite is predominantly alkaline. Plagioclase may be present in small quantities. Syenites are usually peralkaline or peraluminous (Klein & Philpotts, 2013). Any class of intrusive igneous rocks essentially composed of an alkali feldspar and a ferromagnesium mineral is considered a syenite. Syenites contain moderate amounts of silica, relatively large amounts of alkalis, and alumina (Parsons, 1989). They are found in many magmatic terrains or associated with some metamorphic rocks and can form plutons, veins, lenses, and pockets hosted by their parent rocks or a country rock of different composition (Kanouno et al., 2019).

Syenite textures vary from fine to coarse, porphyritic, and even pegmatitic features, highly related to their environment and depth of formation (Kanouo et al., 2019; Mouliom et al., 2022). Alkaline rocks comprise a minor but important component of the continental crust (Manjate, 2017). The origin of alkaline rocks is intimately associated with continental rifts. Alkaline rocks occur in various areas of the world, but in Africa, most nepheline syenites and other alkaline rocks occur within the East African rift system (Chiwona, 2020). Studies show that Neoproterozoic alkaline rocks are concentrated along continental-scale elongate trends (Manjate, 2017). Sporadic alkaline magmatism attests to an extensional environment along the Mozambique belt around 750-450 Ma (Manjate, 2017).

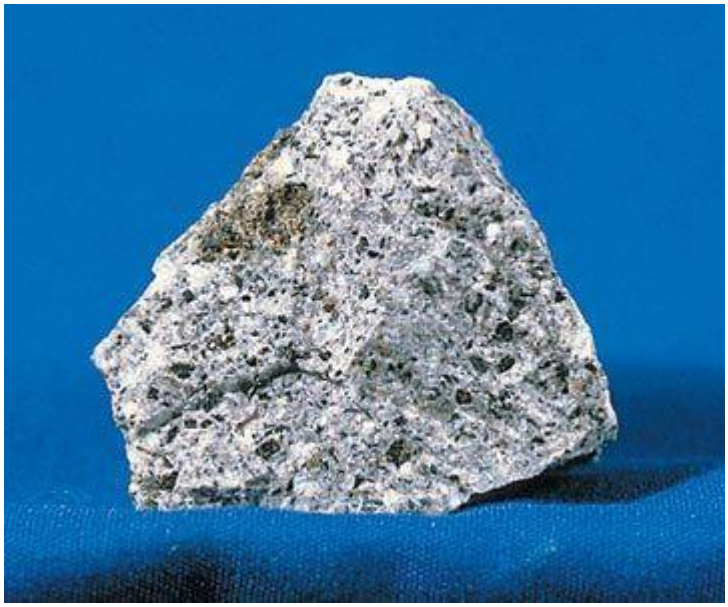


Figure 4: Syenite rock

2.4.2. Gneiss

It is a foliated metamorphic rock identified by its bands and lenses of varying mineral composition. Some of these bands contain granular minerals that are bound together in an interlocking texture (Winter, 2001). Band orientation can be interpreted in terms of stresses that prevailed during the formation of the rock (Liu & Xu, 2015). Quartz and feldspar tend to concentrate in the alternate layers; such rocks are known as gneiss (Philpotts & Ague, 2009). Gneiss is a high-grade metamorphic rock having many of the aerial photograph characteristics of granite (Glass 2013). It is formed by high-temperature and high-pressure metamorphic processes acting on formations composed of igneous or sedimentary rocks (Mishra et al., 2018). Gneiss is usually distinguished from schist by its foliation and schistosity. It is medium to coarse-grained and may contain abundant quartz and feldspar, which some petrographers regard as essential components (Mishra et al., 2018). The mineralogy of a particular gneiss is a result of the complex interaction of protolith composition, pressure, and temperature of metamorphism and addition or loss of components (Chakraborti et al., 2019).



Figure 5: Gneiss rock

2.5. Perthite

Perthite was originally thought to be a single mineral, described at a place near Perth, Ontario, from which its name is derived. Perthite refers to an intergrowth of two feldspar minerals, typically orthoclase and albite, including exsolution processes (Schønwandt et al., 2023). The intergrowth is frequently interpreted as reflecting subsolidus exsolution, but in cases, it can result from a replacement process (Lee & Parsons, 1997). It has been pointed out in many papers that a detailed study of the perthite structure is important for any convincing genetic interpretation (e.g., Alling 1937; Parsons 2010). Perthite gneisses are metamorphic rocks that have undergone high-grade metamorphism, leading to different textures and mineral assemblages. On the other hand, perthitic syenites are intrusive igneous rocks that also contain perthite.

2.6. Regional occurrences of perthitic syenites and perthite gneiss

2.6.1. World

Perthite granite from Masugnsbyn and syenites from Sjaunjatuottar occur in northern Sweden (Gulson 1972). Nepheline sodalite syenites from I.C. Jacobsen Fjord and Ryberg Fjord occur in the southern Blosseville coast, East Greenland (Brooks 1991). They consist largely of perthite with nepheline sodlite salitic pyroxene hastingsiti amphibole sphene and Fe-Ti oxide (Brooks 1991). Braid perthite and micro braid

perthite from Permian nepheline syenite pegmatites in monzonite occur in the Oslo graben in Norway (Ramberg 1972). Perthite in nepheline syenite from the Kakortokite unit occurs in the ilimaussaq complex in south Greenland (Schonwandt et al. 2023). Poikilitic syenites from the Lovozero massif occur in the Kola peninsula in Russia (Mikhailova et al. 2021). Sardasht syenite-monzonite-gabbro appinites intrusions occur in northwest Iran (Fazlnia 2019)

Ultra-high temperature paragneisses from the Qian'an gneiss dome occur in the east Hebei terrane of North China (Liu & Wei 2020). Charnockitic gneisses form part of the Chotanagpur Granite Gneiss Complex in the eastern part of the Peninsular Indian Shield, specifically in the eastern part of the Satpura Mountain Belt of India (Mukherjee et al., 2017). Cambrian orthopyroxene-bearing granitoids and gneisses are found in Dronning Maud Land in Antarctica (Engvik et al. 2024)

2.6.2. Africa

Syenite and granites that are locally overlain by alkaline trachyte and rhyolite and are hosted by Nubian sandstones occur in the El Garra Hamra complex in Egypt (Mahmoud, 2018). The fresh syenites are composed of perthitic K-feldspars, albite, alkali pyroxenes, and secondary alkali amphiboles. Accessory minerals include opaques, apatite, zircon, xenotime, and bastnasite. They were emplaced in a within-plate tectonic setting along the Guinean-Nubian lineament (Mahmoud, 2018). Hydrothermal alteration of the syenites led to extreme enrichment in rare metals as the minerals zircon, gittinsite, bastnasite, parasite, monazite, REE-rich fluorapatite, chevkinite, xenotime, pyrochlore, columbite, Nb-rutile, and thorite (Mahmoud, 2018). Baiebokoum perthite, syenite, and the Passi perthite granulite occur in southern Chad in Africa (Jeremine, 1951). They resemble certain perthitic rocks from the Fennoscandian Shield. Kalsilite nepheline syenites of the Awsard intrusive massif occur in the Reguibat shield, West African craton in Morocco (Haissen et al., 2017). Ina syenite occurs in Linte, central Cameroon (Mouliom et al., 2022). The Ina batholith syenite was assessed for its potential as a feldspar mineral resource for industrial use through petrographic and geochemical characterization (Mouliom et al., 2022). The late pan African Guider syenite pluton occurs in Cameroon (Dawai et al., 2022). It is located on the eastern border of the northwest Cameroon domain is close to the Mayo-Kebbi domain, and is

one of the rare high potassic magmatic bodies in the northern portion of the central African orogenic belt (Dawai et al., 2022)

Granulite facies paragneisses of the Mahamba gneiss complex occur in central Swaziland (Suhr et al., 2014). Mafic granulites and charnockitic gneisses occur in the early Paleozoic domains of northeastern Mozambique (Engvik & Bingen 2016). Abu-Rusheid subsurface gneisses occur in southeastern Egypt (El-Mezayen et al., 2015).

2.6.3. Malawi

Perthosite, a monomineralic saturated syenite of antiperthite, is widespread in the basement complex of southern Malawi and is Precambrian in age (Bose 1961). They are found with banded granulites and amphibolites into which they are observed to merge (Bose 1961). Nepheline syenites occur in Malawi (Chiwona 2020; Dowman et al., 2023). An older and younger set of syenitic rocks can be recognized in the southern Malawi area (Manda 2016). Quartz syenite bodies with nepheline syenite intrusions occur in the Mlindi complex (Chisenga et al., 2021)

Gneiss occurs widely in southern Malawi (Manda 2016). Garnet cordierite gneisses occur in central Malawi (Huang 2017). They display a distinctive perthitic feature observed in the feldspar. Perthosite or perthitic gneiss occurs in the Mlindi complex and is associated with metapyroxenite (Chisenga et al., 2021). Perthite augen gneisses are found in central Malawi (Piper et al., 1989)

2.7. Geochemical studies on syenitic and gneissic rocks

2.7.1. World

Several geochemical studies have been conducted around the world for instance a study was conducted to study whole rock major and trace element data from gneissic granites from the Jitang complex, and the analytical methods used were inductively coupled plasma mass spectrometry (ICPMS), cathodoluminescence images were collected using a Quata 200f scanning microscope, laser ablation, etc. the study showed that the gneissic granites were characterized by high SiO2(Hu et al., 2014). Another study was conducted in Ukraine, the study was on zircons, rock-forming minerals and whole rock compositions of granulite samples from the Bug granulite gneiss complex and the

methods utilized include microprobe REE analysis, secondary to mass spectrometry U-Pb and laser ablation inductively coupled plasma mass spectrometry and the study revealed three major stages in the geological evolution of the complex (Lobach-Zhuchenko et al., 2017). In another study, zircon, U-Pb-Hf isotopes, and geochemistry of Neoarchean dioritic-trondhjemitic gneisses were conducted, and the geochemistry revealed that the dioritic gneisses have low SiO2 contents and various MgO contents, and in contrast, the trondhjemitic gneisses have higher SiO2 and lower MgO contents (Bai et al., 2014). A study on the synthesis of geochemistry and Sm-Nd isotopes of Archean granitoid gneisses in the Jiaodong terrane was conducted, and the study presented new whole-rock geochemical and Sm-Nd isotopic data to constrain the rock's petrogenesis and tectonic setting. The study suggests that the protoliths of most granitoid gneisses are typical tonalitic-trondhjemitic-granodioritic suites (Wu et al., 2014). A study on Zircon U-Pb ages, Hf isotopes, and geochemistry of the schists, gneisses, and granites in the Delbar metamorphic-igneous complex, SE of Shahrood in Iran, was conducted to reveal the geologic history of the complex. A geochemical and U-Pb zircon age characterization study of granites of the Bathani volcano-sedimentary sequence, Chotanagpur granite gneiss complex of eastern India. The study revealed that the granites are of arc magmatism and are interpreted to have formed by partial melting of an igneous source at upper crustal depths (Balaghi Einalou et al., 2014). Studies were conducted on the mineralogy and geochemistry of nepheline syenites from the Bang Phuc Massif of the alkaline Chon Don complex in northeastern Vietnam. The study showed that the nepheline syenites formed through fractional crystallization of pristine mantle-derived basaltic melt modified by subduction-related components, as shown by the geochemical data, and the study helped gain insights into the geologic history of the complex (Balaghi Einalou et al., 2014). The bulk rock geochemistry of granitoids from the Chotanagpur granite gneissic complex was conducted, and the data obtained suggest that the augen gneiss has been derived from a hybrid source involving older crustal rocks and metasomatized mantle, and the protolith of the augen gneiss was emplaced in an early Paleoproterozoic basement in a continental arc setting (Mukherjee et al., 2019).

2.7.2. Africa

In Africa, several studies have been conducted. For example, the tectonic setting of the syenite around Igarra, southwestern Nigeria, was studied. The sampling was carried out using the survey-type geological field approach. The composition was intermediate in regards to SiO2, having AL2O3 and alkali compositional ranges, and the trace and REE concentrations are similar and consistent. The syenites are high K calc-alkaline, alkalic to alkalic-calcic (Ugbe et al., 2023).

2.7.3. Malawi

In Malawi, a study conducted on geophysical and geochemical characterization of apatite mineralization on Mlindi ring structure by (Chisenga et al., n.d.), the geochemical and magnetic data of the Mlindi ring structure have been used to understand the full extent of rare earth and base metal mineralization hosted in the apatite-rich meta pyroxenite and other mafic or ultramafic rocks. A study was conducted on the petrology and geochemistry of selected nepheline syenites from Malawi and their potential as alternative potash sources by (Chiwona et al., 2020) this study was conducted to assess these nepheline syenites, especially within the Chilwa alkaline province, they used airborne geophysical gamma-ray data acquired in 2013, coupled with satellite remote sensing to identify nepheline syenites. The results indicate that the nepheline syenites from Malawi have similar geochemistry and mineralogical composition to those that have been used as crushed rock fertilizers in other parts.

2.8. Metamorphism and magmatic differentiation of syenitic and gneissic rocks

The formation of syenitic and gneissic rocks involves complex interplay between magmatic differentiation and metamorphic processes such as orogenic collisions, continental rifting, and high-grade metamorphism (Luan et al, 2019). These processes are crucial for understanding the petrogenesis of perthitic syenites and perthite gneiss at Thyolo mountain, which lie within the tectonically active Mozambique belt and the southern extension of the EARS

2.8.1. Magmatic Differentiation of syenitic rocks

Syenites are coarse-grained, intrusive rocks primarily composed of alkali feldspars, with minor plagioclase, quartz, and mafic minerals (Klein & Philpotts, 2013). Their formation is typically associated with magmatic differentiation in silica oversaturated to

undersaturated, often extensional or post-orogenic tectonic settings (Kanouo et al, 2019; Hurai et al, 2010; Xiao, 2005). Magmatic differentiation involves processes such as fractional crystallization, magma mixing, and assimilation, which govern the mineralogical and geochemical evolution of syenitic melts

Fractional crystallization

Syenites commonly form through the progressive crystallization of alkali magmas, where early crystallization of mafic minerals enriches the residual melt in alkalis and silica (Winter, 2001). This process is evident in alkaline syenites of the East African rift system, where nepheline syenites, syenites show enrichment in large ion lithophile elements (LILE) like Ba and Sr due to the removal of mafic phases (Chiwona et al., 2020). Perthitic textures characterized by exsolution of albite in K-feldspar form during slow cooling below the feldspar solvus, ~700 °C, indicating deep crustal crystallization (Parsons, 2010)

2.8.2. Magma source and tectonic setting

Syenitic magmas are often derived from partial melting of metasomatized mantle or lower crustal material in continental rift zones or post-orogenic environments (Manjate, 2017). In the Chilwa alkaline province (CAP) of southern Malawi, syenites are linked to Jurassic-Cretaceous rifting, with magmas generated in an extensional regime associated with EARS (Nyalugwe, 2019). Globally, syenites in the Oslo Graben, Norway, and Ilimaussaq complex in Greenland illustrate similar rift-related origins, with perthitic syenites forming from differentiated alkaline melts (Schonwandt et al., 2023)

Perthite formation

The perthitic texture in syenites results from subsolidus exsolution, where cooling of a homogeneous alkali feldspar leads to phase separation in K-rich orthoclase and Na-rich albite lamellae (Lee & Parsons, 1997). Perthite formation reflects slow cooling and is a key diagnostic feature for distinguishing syenites from other igneous rocks

2.8.3. Metamorphism of Gneissic rocks

Gneisses are high-grade metamorphic rocks characterized by foliation banding and interlocking mineral textures formed under amphibolite to granulite facies conditions (Philpotts & Ague, 2009). They typically derive from igneous or sedimentary protoliths

subjected to high temperature (>600C °C) and pressure (>0.5 GPa), with mineral assemblages including quartz, feldspar, and mafic minerals (Mishra et al, 2018). Perthite gneiss, like that at Thyolo mountain, contains perthitic feldspars, indicating complex metamorphic and recrystallization processes

2.8.4. Metamorphic processes

Gneiss formation involves recrystallization, deformation, and partial melting (migmatization) under high-grade conditions. In the Mozambique belt, gneisses are products of Neoproterozoic Cambrian collisions during the pan African orogeny, where mafic to felsic protoliths underwent amphibolite to granulite facies metamorphism (Tsunogae et al., 2021). Migmatization, common in the Malawi basement complex, produces perthitic textures through recrystallization of feldspars under high temperature conditions (Carter & Bennett, 1973)

2.8.5. Perthite in Gneisses

Perthite in gneisses forms through metamorphic recrystallization or exsolution during cooling from peak metamorphic conditions. In high-grade metamorphism, feldspars may homogenize at elevated temperatures and exsolve into perthitic intergrowths upon cooling, as seen in charnockitic gneisses of the Chotanagpur granite gneiss complex, India (Mukherjee et al., 2017). In Malawi, perthitic textures are enhanced by pan-african metamorphism or later EARS-related deformation (Huang, 2017)

2.8.6. Tectonic setting

Gneiss in the Mozambique belt reflects polyphase metamorphism with early events like the irumide orogeny 1.0 Ga overprinted by the pan-african pan-african orogeny 800-550 Ma (Manda et al., 2018). The proximity of the Thyolo to the EARS suggests additional low-grade metamorphic overprinting due to rift-related faulting as evidenced by the Thyolo fault scarp (Wedmore et al., 2020)

2.9. Economic and industrial significance of perthitic syenites and perthite gneiss

The geological characteristics of syenites and their deposits make them an industrial mineral exploited for economic and strategic purposes worldwide (Mouliom et al., 2022; Kanouo et al., 2019). Syenites are used as freestone, potash for soil enrichment, gold, rare earth elements, filler in paint industries, and feldspathic flux in ceramic and glass (Mouliom et al., 2022). Syenites are used for flooring, homes, hotels, and interior

decoration, building stone as a facing stone or paving stone for garden decoration or the purposes of office building, curbing purposes, dimension stone, cement manufacturing, construction or road aggregate, for landscaping, manufacturing natural cement and magnesium and dolomite refractories, artefacts, monuments, sculpture, small figurines, cemetery markers and various artwork (Mahadevan & Sathapathi, 1954; Mouliom et al., 2022). Syenites are very good in the mining and processing industries as they can host gemstones and ore minerals, enrich soil profiles with minable metallic elements (Kanouo et al., 2019). Gem-quality corundum was discovered in some syenites in the Cerova Mountains, Slovakia, and the Ilmen Mountains, South Ural, Russia (Uher et al., 2006; Sorokina et al., 2017). Rare earth elements have been reported in the Misy syenitic intrusion in northern Quebec, Canada, and the Maoniuping carbonatite syenite complex in Sichuan province, China (Petrella et al., 2014; Xu et al., 2004). Gold mineralization was found in young-Davidson syenites, Matachewan, Ontario, and Abitibi syenites in Canada (Zhang et al., 2014; Bigot & Jebrak, 2015). Uranium ore was found in agpaitic nepheline syenites in Greenland (Sorensen et al., 2011). Iron ore deposits were characterized in syenites found in Greenland (Bogva, 1950).



Figure 6: nepheline syenite ceramic flour (Bhoomi Pottery https://www.bhoomipottery.com/products/laguna-clay-nepheline-syenite-a-270-india)

Metamorphic gneiss has many uses, like flooring, ornamental stones on buildings, and work surfaces, facing stones on gravestones (Bonewitz, 2012). Gneiss usually resists fracturing along planes of weakness, like many other metamorphic rocks, thus allowing for applications in road construction and landscaping (Klein & Philpotts 2017; Cavallo et al 2022). It is long-lasting, therefore utilized in paving and curbing. Some gneisses are vibrantly polished and used as architectural stone, beautiful floor tiles, facing stone, stair treads, window sills, counter tops, and cemetery monuments (Cavallo et al., 2022).

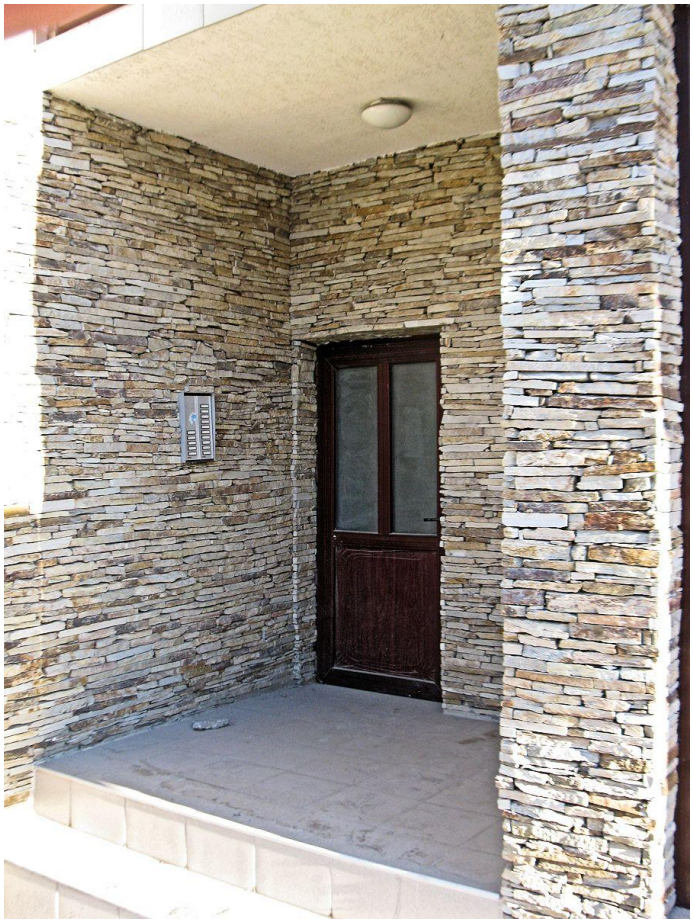


Figure 7: gneiss wall decoration

Perthite is of industrial interest due to its applications in construction, manufacturing glass and ceramics, and gemstones in rare cases, e.g., in moonstone varieties (Sedawie,

2023; Nesse, 2000; Hall, 1987). Perthite gemstones include amazonite, rainbow lattice sunstone, and moonstone (Sedawie, 2023).

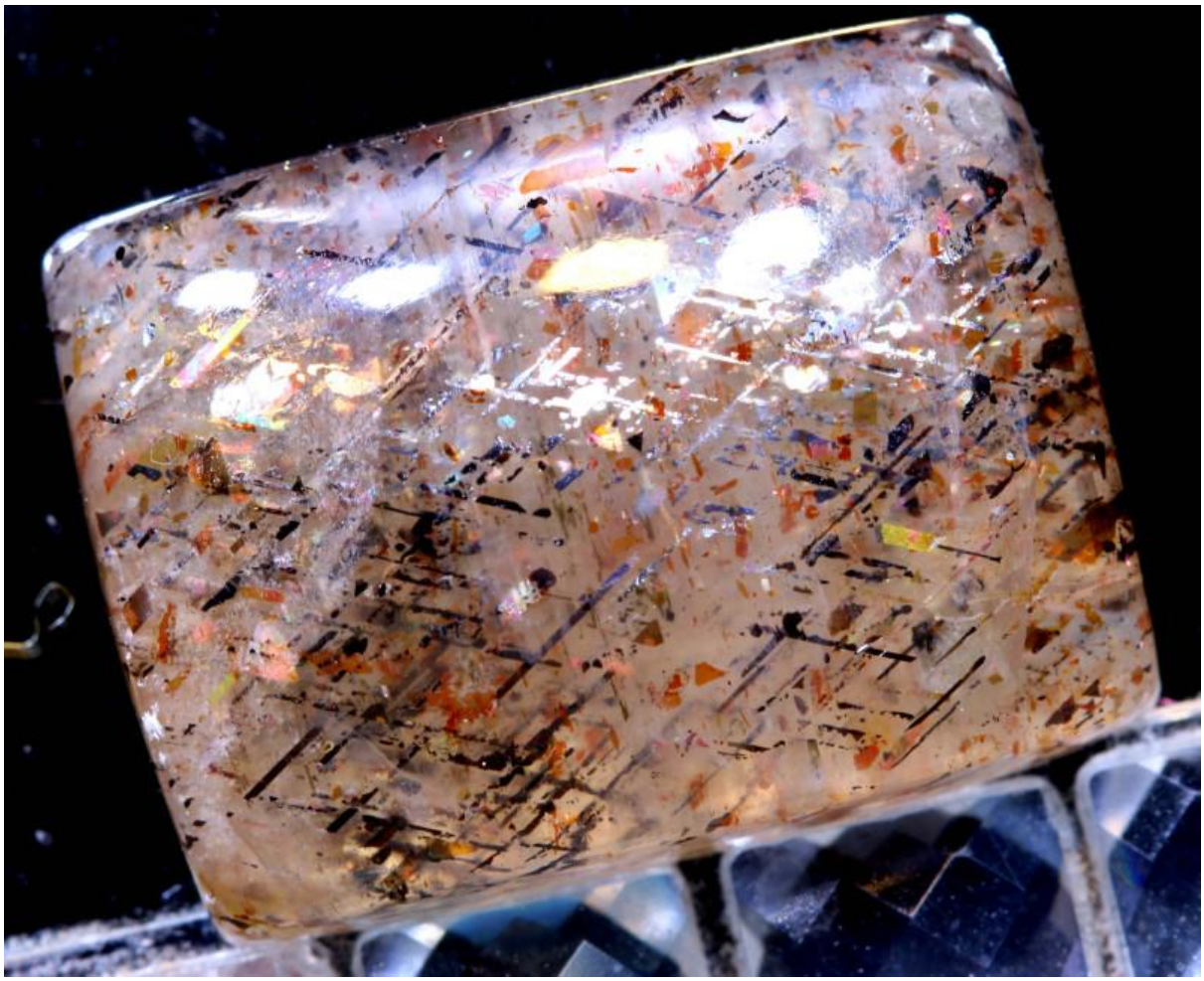


Figure 8: Rainbow lattice sunstone

2.10. Knowledge gaps and justification for the study

2.10.1. Petrogenesis

Features presented by syenites are useful for the identification and differentiation of syenitic rocks and can also help to understand the conditions under which rocks formed (Kanouno et al., 2019). Syenites present distinctive petrography and geochemical features important in differentiating them and their characterisation. They are useful in constraining crystallisation history, including petrogenesis and tectonic setting (Kanouno et al., 2019). The study provides an opportunity to add to the geological data of southern Malawi. According to Albarède (2009), geochemistry is used to understand several terrestrial and planetary processes. It will also be used to acquire an enhanced geological understanding of the area. Through comprehensive geochemical data, an

enhanced understanding of the formation, evolution, and metamorphic history of the perthite gneisses and perthitic syenites. Chemical elements are the building blocks of any physical material, including rocks and minerals (Alexandre, 2021). Thus, analysing major and trace elements, including rare earth elements, helps delineate the petrogenesis of these rocks, and comparing the geochemical characteristics of Thyolo hill rocks with other formations in the region will help understand the regional geology of the area. This investigation provides an opportunity to investigate the crystallisation history, petrogenesis, and tectonic setting of Thyolo Mountain.

Burke et al. (2003) suggested that repeated episodes of alkaline magmatism in southeast Africa could point to the location of pan African suture zones. This model is very speculative. Testing Burke et al., (2003) suture zone hypothesis could contribute to Gondwana reconstruction debates

2.10.2. Economic rationale

Syenitic rocks are very good in mining and processing industries and can host gemstones and ore minerals, or can enrich soil profiles with some minable metallic elements, and can also be mined as industrial minerals or raw materials for some industries (Kanouno et al., 2019). Geochemical knowledge and tools are used to discover mineral deposits that are in the subsurface (Alexandre, 2021). The detailed geochemical analysis thus can identify economically significant minerals within the perthite gneisses and perthitic syenites. Geochemical exploration is used to understand how deposits form and under what conditions; thus, geochemistry is a powerful tool (Alexandre, 2021). Geochemical data could reveal industrial minerals supporting Malawi's resource development.

2.10.3. Environmental impact

Understanding the geochemical composition of rocks and their weathering products helps assess their impacts on soil and water quality. Geochemistry is used to distinguish processes that operate at low temperatures at the Earth's surface and in which there are interactions between rocks (Misra, 2012), the atmosphere, the hydrosphere, and the organisms that inhabit them (Rollinson & Pease, 2021). Thus, the study can inform environmental management organisations by identifying potential sources of contamination and helping develop ways to mitigate environmental impacts. This is crucial for agriculture, drinking water safety, and overall ecosystem health.

Chapter 3 Methodology

3.1. Research design

A quantitative approach research design was used. A preliminary desk study and literature review were conducted to help gather information about the area from various sources. Remote sensing in the form of satellite images from the United States Geological Survey Earth Explorer and Copernicus was used to study the area further to help understand the area further.

3.2. Geological Survey

A geological survey and characterisation of syenites and gneiss were conducted on Thyolo Mountain. Outcrops were described based on the following parameters: colour, texture, structure, weathering, and mineralogical composition. A hand lens was used to observe rock samples. A silver compass was used to determine the dip and strike of the outcrops sampled. A handheld Garmin global positioning system device was used to accurately determine the geographical coordinates of the points sampled. This process would not have been achieved without the help of the locals, namely Justin Sausten, Lucky Kampira, Chimwemwe Henry, and Samson Makombola, who humbly acted as field assistants and guides throughout the whole survey

Table 1: Data collected during the survey

T/A	Village	Sample ID	X	Y	Elevation (m)	Description
Samuyele	Kali Ntulo	TH 1	718419	8224373	1177	coarse-grained, slightly weathered, pinkish, and dark crystal grains,
		TH 2	718319	8224362	1166	similar lithology to TH 1, small intrusions into the rock, visible chemical weathering

		TH 3	718807	8225227	1064	fractured igneous rock, leucocratic, coarse-grained, light and dark mineral grains, found on a farm
		TH 4	718347	8225108	1093	massive outcrop, light and coloured mineral grains, fractured, brown soil, chemical weathering
		TH 5	718052	8224406	1202	massive outcrop, greyish igneous rock, light and dark mineral grains, minimal weathering
		TH 6	718059	8224288	1217	chemical weathering, greyish igneous rock, coarse-grained, massive outcrop, intrusion, plagioclase
Mphuka	Kali Ntulo 2	TH 7	717804	8224649	1174	big outcrop, coarse-grained, fractures, chemical weathering, light and dark mineral grains
		TH 8	717754	8224303	1213	chemical weathering, greyish igneous rock, found in farmland
		TH 9	717642	8224121	1231	coarse-grained, slightly weathered, fractured, greyish rock, medium outcrop, mainly dark mineral grains
		TH 10	717586	8224031	1238	big outcrop, coarse-grained, light and dark mineral grains, intrusions, large feldspars,
		TH 11	717209	8223804	1242	outcrop, greyish colour, light and dark mineral grains, intrusions, slightly weathered
		TH 12	717103	8223836	1235	outcrop, coarse-grained igneous rock, slightly weathered, fractures, greyish

		TH 13	716948	8223744	1232	small widespread rocks, dark mineral grains, coarse-grained, metamorphic?
		TH 14	716947	8223978	1222	outcrop, light grey, coarse mineral grains, intrusion, slightly weathered
		TH 15	716799	8224056	1214	coarse-grained, dark grey minerals, slightly weathered, hard rock, near farmland
		TH 16	716770	8224017	1214	small outcrop, greyish, coarse-grained, slightly weathered, in farmland
		TH 17	716574	8223988	1208	very big outcrop, coarse-grained, fractured, intrusions, dark and light-coloured mineral grains
		TH 18	716611	8223959	1210	buried outcrop, coarse-grained, weathered, fractured, light and brown mineral grains
		TH 19	716460	8224068	1204	big outcrop, chemical weathering, fractured, intrusions, dark and light pinkish brown mineral grains
		TH 20	716474	8224204	1204	big outcrop, phenocrysts visible, intrusions, majority dark coloured crystals, near Inkhathi stream or river
		TH 21	717190	8224584	N/A	big outcrop, coarse-grained, intrusions, dark and light brownish mineral grains, chemical weathering
		TH 22	717225	8224791	1177	dark and light mineral grains, intrusions, big outcrop, chemical weathering



Figure 9: Tools used during the survey

3.3. Sampling and Analysis

Representative rock samples were collected from outcrops of the Thyolo mountain using a geological hammer. 22 rock samples were collected on a total of 20 outcrops. The collected samples were macroscopically described, thin-sectioned, microscopically characterised, and geochemically analysed. 5 thin sections were prepared at the Geological Survey (GSD) in Zomba, photographed at the University of Malawi (UNIMA), and observed at the Malawi University of Science and Technology (MUST) in Thyolo. Rock powders from 12 samples were prepared. Their major, minor, trace, and rare earth element contents were determined at a geological survey in Zomba. Fresh rock samples were cleaned, crushed. Elemental compositions of the samples were determined using X-ray fluorescence (XRF) spectrometry.

Table 2: X-ray Fluorescence data received from the Geological Survey

Element	TH 3	Th 4	TH 5	TH 7	TH 9	TH 11	TH 12	TH 13	TH 15	TH 18	TH 21
Na2O	3.11 %	2.70 %	2.91 %	2.94 %	3.05 %	3.42 %	3.34 %	1.13 %	0.53 %	3.09 %	3.09 %
MgO	1.60 %	3.24 %	2.87 %	1.96 %	2.63 %	3.19 %	3.61 %	4.03 %	4.69 %	0.35 %	2.28 %
Al2O3	12.76%	14.38%	13.42%	14.89%	12.33%	14.86%	13.73%	14.20%	16.95%	11.64 %	13.74%
SiO2	47.12%	51.10 %	54.34%	54.86%	52.02%	54.74%	48.55%	44.38%	39.39%	62.64%	54.21%
P2O5	0.48 %	1.15 %	0.72 %	0.82 %	0.88 %	1.22 %	1.27 %	0.20 %	0.94 %	0.17 %	0.65 %
SO3	0.05 %	0.03 %	0.03 %	0.03 %	0.03 %	0.02 %	0.04 %	0.07 %	0.06 %	0.02 %	0.02 %
Cl	0.11 %	0.05 %	0.15 %	0.14 %	0.11 %	0.14 %	0.12 %	0.01 %	0.02 %	0.02 %	0.11 %
K2O	6.30 %	5.21 %	5.50 %	6.10 %	6.08 %	6.21 %	5.52 %	0.76 %	0.73 %	3.70 %	5.73 %
CaO	3.36 %	4.52 %	3.35 %	3.53 %	4.24 %	4.82 %	4.02 %	9.73 %	8.24 %	1.13 %	3.80 %
TiO2	10280ppm	7542ppm	8133 ppm	10740ppm	9062ppm	12500ppm	9497ppm	6141 ppm	8048ppm	5428ppm	9365ppm
V	97.5 ppm	82.2 ppm	81.1ppm	103.5ppm	96.2 ppm	123.8ppm	99.0 ppm	277.1ppm	288.4ppm	39.4 ppm	88.1 ppm
Cr	161.9 ppm	151.7 ppm	122.0ppm	125.1 ppm	129.9ppm	171.6 ppm	109.4ppm	125.6ppm	254.4ppm	168.2ppm	150.2ppm

MnO	611.1ppm	684.0ppm	692.7ppm	735.3ppm	1013ppm	916.6ppm	554.9ppm	1695ppm	1379ppm	223.9ppm	695.4ppm
Fe2O3	4.93%	5.01%	4.64%	5.72%	5.16%	6.41%	4.99%	11.45%	11.54%	2.31%	5.27%
Co	9.0ppm	<0.4ppm	<0.4ppm	11.2ppm	14.9ppm	<0.4ppm	<0.3ppm	<0.4ppm	<0.3ppm	<0.3ppm	<0.4ppm
Ni	29.3ppm	64.0ppm	44.7ppm	40.2ppm	55.6ppm	57.1ppm	58.0ppm	62.0ppm	88.4ppm	9.8ppm	52.9ppm
Cu	14.0ppm	1.7ppm	11.7ppm	34.9ppm	17.4ppm	13.9ppm	6.0ppm	145.2ppm	126.8ppm	8.8ppm	11.5ppm
Zn	79.0ppm	56.4ppm	77.1ppm	105.8ppm	90.6ppm	102.8ppm	74.1ppm	73.7ppm	86.6ppm	21.6ppm	80.4ppm
Ga	22.0ppm	17.1ppm	18.8ppm	21.1ppm	19.5ppm	21.7ppm	19.2ppm	12.8ppm	14.2ppm	20.8ppm	20.7ppm
Ge	0.6ppm	0.5ppm	0.6ppm	0.7ppm	0.7ppm	0.7ppm	0.5ppm	<0.3ppm	<0.3ppm	0.6ppm	0.7ppm
As	3.8ppm	1.1ppm	2.6ppm	3.9ppm	3.0ppm	4.2ppm	2.2ppm	<0.2ppm	<0.2ppm	0.9ppm	5.1ppm
Se	<0.1ppm	<0.1ppm	<0.1ppm	<0.1ppm	<0.1ppm	<0.1ppm	<0.1ppm	<0.1ppm	<0.1ppm	<0.1ppm	<0.1ppm
Br	2.4ppm	0.6ppm	3.6ppm	0.7ppm	3.1ppm	4.1ppm	1.9ppm	<0.2ppm	<0.2ppm	1.7ppm	3.7ppm

Rb	166.1 ppm	89.3 ppm	142.3ppm	168.3ppm	141.6 ppm	150.2ppm	123.6ppm	24.4 ppm	25.3 ppm	87.4 ppm	153.3ppm
Sr	1326 ppm	2353ppm	1408 ppm	1709 ppm	1796 ppm	1522 ppm	1799 ppm	141.3 ppm	122.0ppm	741ppm	1482 ppm
Y	18.9 ppm	16.9 ppm	19.2 ppm	29.4 ppm	21.6 ppm	29.2 ppm	23.6 ppm	20.5 ppm	21.9 ppm	0.6ppm	24.1 ppm
Zr	513.5ppm	108.7ppm	235.3ppm	467.9ppm	436.2ppm	449.6ppm	87.5 ppm	93.1 ppm	83.9 ppm	424.1ppm	297.1ppm
Nb	23.1 ppm	5.8ppm	15.2 ppm	30.1 ppm	15.5 ppm	27.1 ppm	12.6 ppm	6.1ppm	6.5ppm	13.2 ppm	23.1 ppm
Mo	7.8ppm	2.3ppm	5.3ppm	6.3ppm	5.7ppm	4.0ppm	3.0ppm	1.2ppm	<0.1 ppm	9.7ppm	6.3ppm
Ru	<0.2ppm	<0.2ppm	<0.2ppm	<0.2 ppm	<0.2ppm	<0.2 ppm	<0.2ppm	<0.2ppm	<0.2ppm	<0.2ppm	<0.2ppm
Rh	<0.3ppm	<0.2ppm	<0.2ppm	<0.2 ppm	<0.2ppm	<0.2 ppm	<0.2ppm	<0.2ppm	<0.2ppm	<0.2ppm	<0.2ppm
Pd	<0.2 ppm	<0.2ppm	<0.2ppm	<0.2 ppm	<0.2ppm	<0.2 ppm	<0.2ppm	<0.2ppm	<0.2ppm	<0.2ppm	<0.2ppm
Ag	1.6ppm	1.9ppm	1.7ppm	1.6ppm	1.5ppm	1.1ppm	1.6ppm	1.2ppm	1.7ppm	1.5ppm	1.3ppm
Cd	<0.2 ppm	<0.2ppm	<0.2ppm	<0.2 ppm	<0.2ppm	<0.2 ppm	<0.2ppm	<0.2ppm	<0.2ppm	<0.2ppm	<0.2ppm
In	<0.3 ppm	<0.3ppm	<0.3ppm	<0.3 ppm	<0.3ppm	<0.3 ppm	<0.3ppm	<0.3ppm	<0.3ppm	<0.3ppm	<0.3ppm

Sn	2.3ppm	<0.7ppm	<0.7ppm	1.0ppm	<0.7ppm	1.1ppm	<0.7ppm	<0.2ppm	<0.7ppm	1.4ppm	1.1ppm
Sb	2.6ppm	<0.4ppm	<0.4ppm	<0.4ppm	1.5ppm	1.0ppm	<0.4ppm	<1.1ppm	<0.4ppm	2.4ppm	<0.4ppm
Te	9.0ppm	2.9ppm	2.4ppm	4.6ppm	7.9ppm	9.6ppm	<0.5ppm	3.9ppm	2.3ppm	7.5ppm	6.2ppm
I	16.8ppm	8.1ppm	8.7ppm	10.1ppm	12.1ppm	13.9ppm	2.6ppm	10.2ppm	8.4ppm	14.6ppm	11.1ppm
Cs	39.4ppm	21.3ppm	24.2ppm	29.4ppm	31.9ppm	36.0ppm	10.7ppm	25.2ppm	20.5ppm	35.0ppm	26.9ppm
Ba	2355ppm	4593ppm	3070ppm	3454ppm	3157ppm	2905ppm	3664ppm	354.5ppm	408.9ppm	1234ppm	2662ppm
La	163.5ppm	130.6ppm	150.3ppm	166.1ppm	163.7ppm	172.6ppm	119.4ppm	69.8ppm	70.2ppm	104.0ppm	162.5ppm
Ce	239.3ppm	191.3ppm	228.0ppm	275.8ppm	241.0ppm	278.7ppm	179.3ppm	87.8ppm	82.6ppm	132.5ppm	264.3ppm
Pr	<1.0ppm	31.4ppm	28.3ppm	32.3ppm	31.3ppm	40.2ppm	23.4ppm	37.9ppm	39.5ppm	31.7ppm	41.9ppm
Nd	152.0ppm	116.7ppm	124.5ppm	158.6ppm	147.5ppm	175.3ppm	130.1ppm	54.1ppm	58.6ppm	80.9ppm	161.2ppm
Sm	1.9ppm	<1.5ppm	<1.5ppm	<1.5ppm	<1.5ppm	<2.1ppm	<1.5ppm	<1.5ppm	<1.5ppm	<1.5ppm	<1.5ppm
Yb	<0.4ppm	<0.3ppm	<0.3ppm	<2.7ppm	<0.4ppm	<0.4ppm	<0.3ppm	<3.4ppm	<3.7ppm	<0.3ppm	<0.3ppm

Hf	9.4ppm	<1.2ppm	1.8ppm	8.1ppm	8.0ppm	8.9ppm	<1.2ppm	<2.5ppm	<2.4ppm	9.6ppm	5.5ppm
Ta	<0.8ppm	<0.8ppm	<0.8ppm	3.2ppm	<0.8ppm	<0.8ppm	<0.8ppm	14.8ppm	8.9ppm	<0.8ppm	2.1ppm
W	2.3ppm	0.9ppm	2.7ppm	1.5ppm	3.2ppm	3.2ppm	2.2ppm	<0.5ppm	<0.5ppm	1.4ppm	3.1ppm
Au	<0.1ppm	<0.1ppm	<0.1ppm	<0.1ppm	<0.1ppm	<0.1ppm	<0.1ppm	<0.1ppm	<0.1ppm	<0.1ppm	<0.1ppm
Hg	<0.1ppm	<0.1ppm	<0.1ppm	<0.1ppm	<0.1ppm	<0.1ppm	<0.1ppm	<0.1ppm	<0.1ppm	<0.1ppm	<0.1ppm
Ti	<0.2ppm	<0.2ppm	<0.2ppm	<0.2ppm	<0.2ppm	<0.2ppm	<0.2ppm	<0.2ppm	<0.2ppm	<0.2ppm	<0.2ppm
Pb	49.6ppm	30.6ppm	48.2ppm	68.1ppm	44.6ppm	47.1ppm	40.5ppm	1.6ppm	3.3ppm	36.2ppm	47.6ppm
Bi	<0.3ppm	<0.3ppm	<0.3ppm	<0.3ppm	<0.3ppm	<0.3ppm	<0.3ppm	<0.3ppm	<0.3ppm	<0.3ppm	<0.3ppm
Th	7.7ppm	1.8ppm	3.4ppm	7.3ppm	5.5ppm	6.5ppm	3.2ppm	2.6ppm	4.1ppm	11.6ppm	14.8ppm
U	1.1ppm	<0.3ppm	<0.3ppm	1.6ppm	<0.3ppm	<0.3ppm	<0.3ppm	<0.4ppm	<0.3ppm	<0.3ppm	1.4ppm

SAMPLING POINT MAP

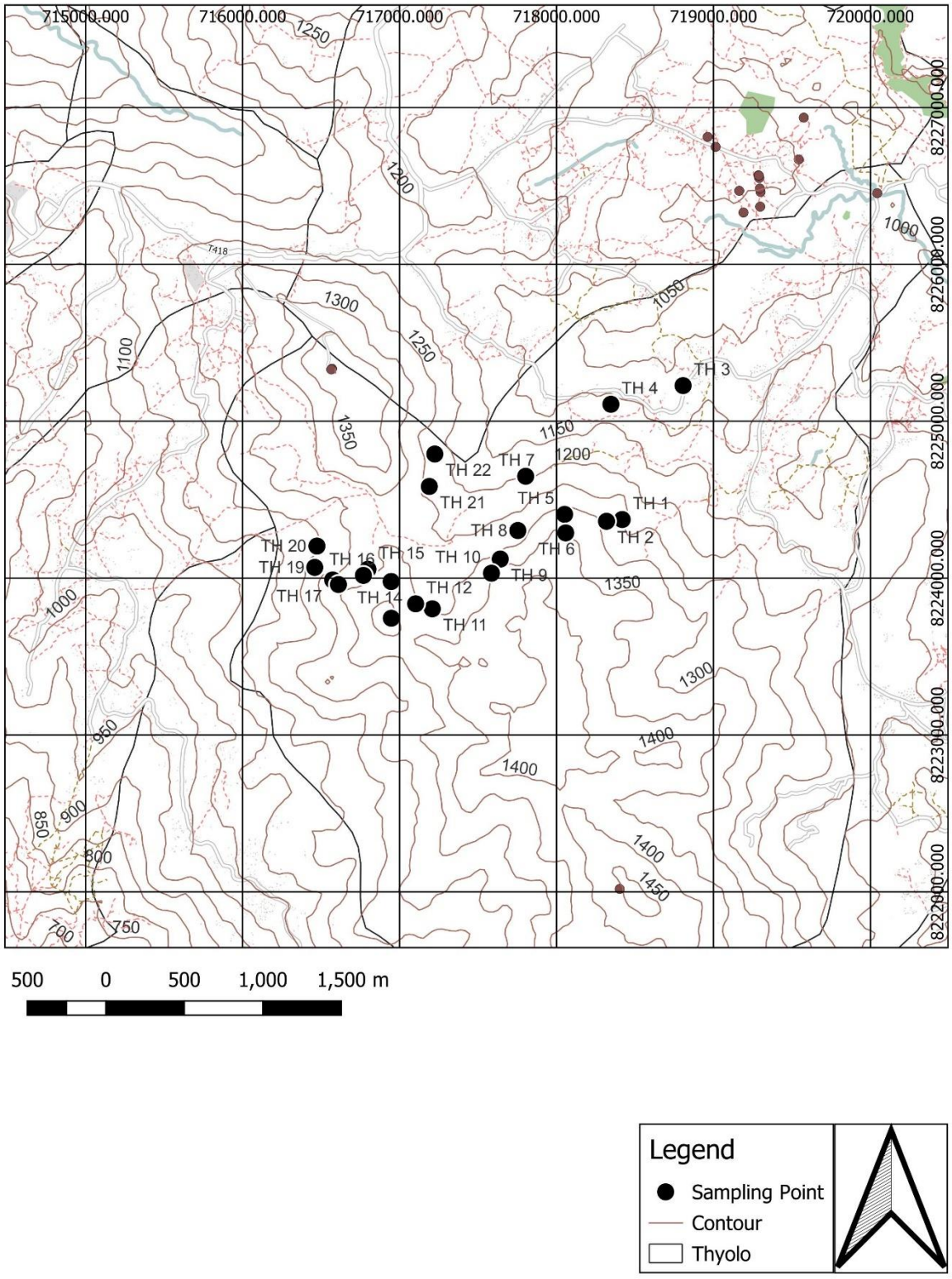


Figure 10: Sampling Point Map of the Thyolo mountain

Statistical Analysis

Principal component analysis (PCA) and K-means clustering were applied to trace element data to help identify patterns. Statistical analysis was conducted using RStudio

Chapter 4 Results and Discussions

4.1. Geochemistry

Major Elements: Normalised major oxides show a range of compositions for the Thyolo Mountain rock samples. SiO2 ranges from 46.92 wt.% to 73.19 wt.%, indicating a variety of intermediate to felsic compositions. The majority of rocks sampled are observed to be around the ranges of 56 to 61 wt.% of SiO2, typical of syenites (Watkins & Roex, 1991). The high value of SiO2 in TH 18 suggests a more granitic nature, and the lower value for TH 15 suggests a more mafic composition.

Table 3: Normalized Major oxides of samples from Thyolo Mountain

Sample ID	TH 3	TH 4	TH 5	TH 7	TH 9	TH 11	TH 12	TH 13	TH 15	TH 18	TH 21
Na2O	3.846411	3.062674	3.281124	3.201071	3.488686	3.554961	3.858483	1.299478	0.631314	3.610307	3.446189
MgO	1.977694	3.676571	3.23712	2.127886	3.003542	3.311726	4.17049	4.646267	5.581768	0.405196	2.542873
Al2O3	15.80174	16.31762	15.14191	16.1902	14.10807	15.44641	15.86612	16.38773	20.19013	13.59999	15.30402
SiO2	58.3525	57.98542	61.31233	59.65039	59.52163	56.90016	56.10343	51.21742	46.91972	73.18758	60.3807
P2O5	0.59628	1.299282	0.815316	0.891276	1.004957	1.265025	1.469898	0.230928	1.120403	0.201313	0.72321
K2O	7.803037	5.913151	6.20683	6.632653	6.960209	6.45506	6.383426	0.875359	0.869069	4.326526	6.378902

CaO	4.164674	5.129043	3.778708	3.84259	4.851436	5.015436	4.643122	11.22444	9.818718	1.314432	4.23478
TiO2	1.273055	0.855824	0.915397	1.167782	1.03688	1.299328	1.097455	0.708712	0.958644	0.634199	1.043101
MnO	0.075677	0.077616	0.078158	0.079951	0.115908	0.095215	0.641232	0.195614	0.164261	0.02616	0.077456
Fe2O3	6.108932	5.682798	5.233099	6.216209	5.908683	6.657755	5.765346	13.21405	13.74597	2.694294	5.868768

The high K2O and Na2O composition of the samples confirms the alkaline nature, typical of syenites (Kanouo et al., 2019). The total alkali silica diagram plots most of the samples in the syenite or quartz syenite field. On the other hand, TH 18 plots are near granite fields. This confirms the presence of perthitic syenites, as alkali feldspar is a typical sign of these rocks (Deer et al., 2013). The plotted data SiO2 versus Na2O + K2O diagram distinguishes syenites, granites, and gneisses.

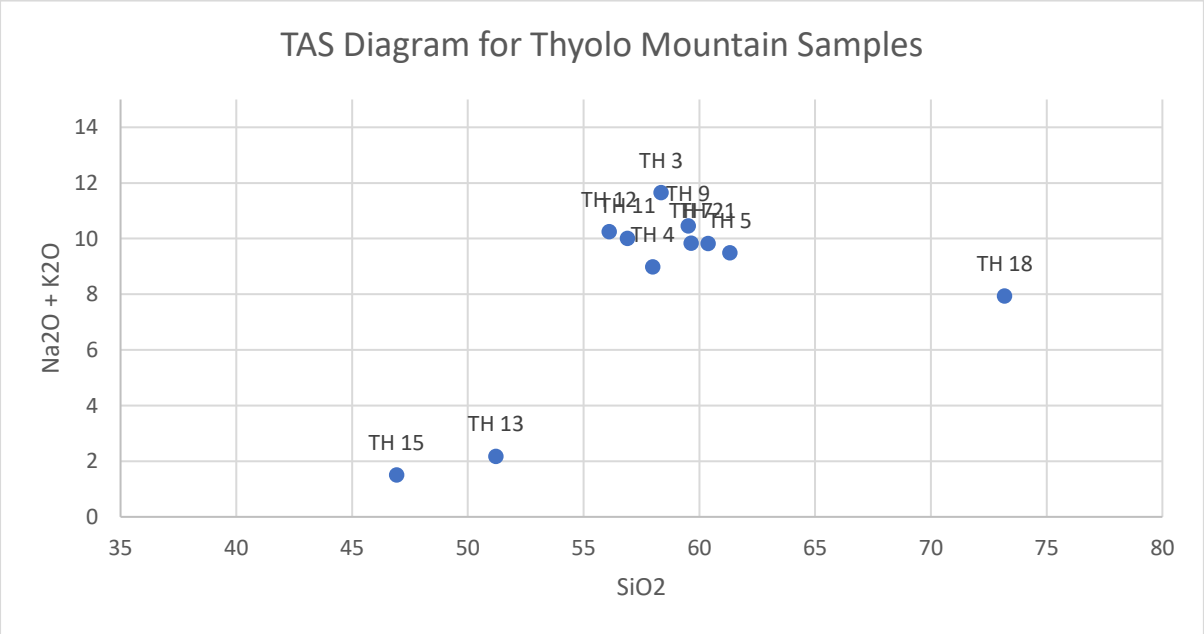
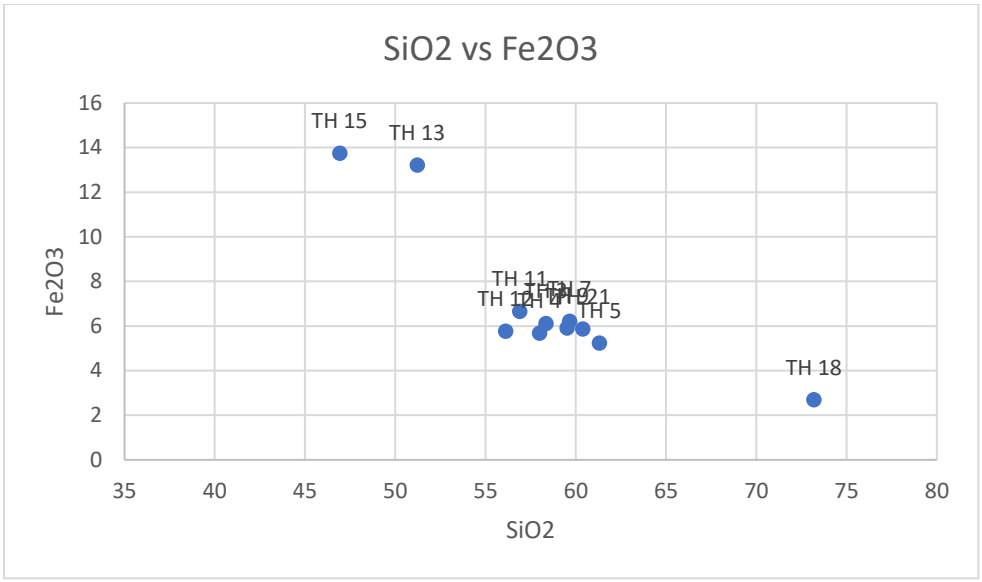
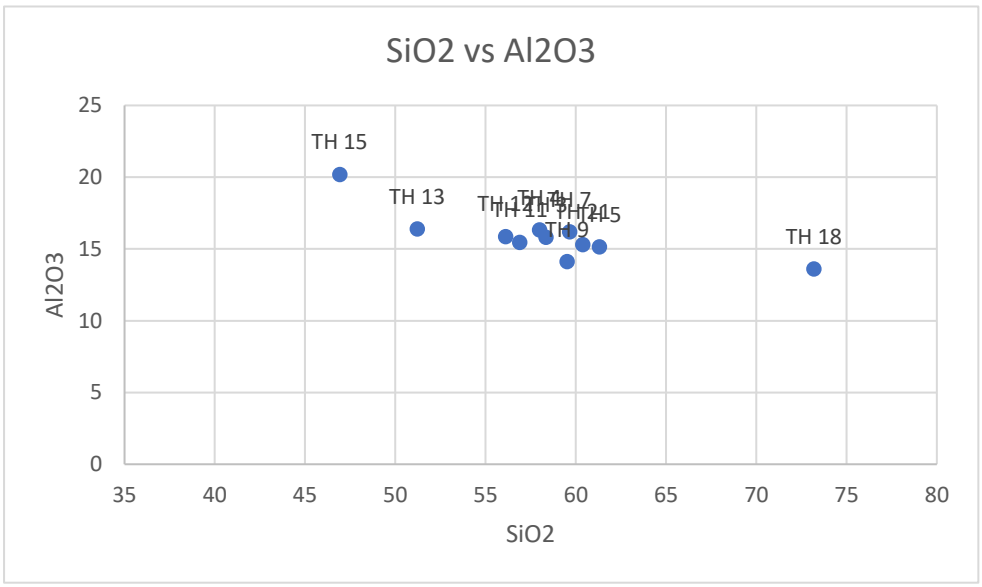
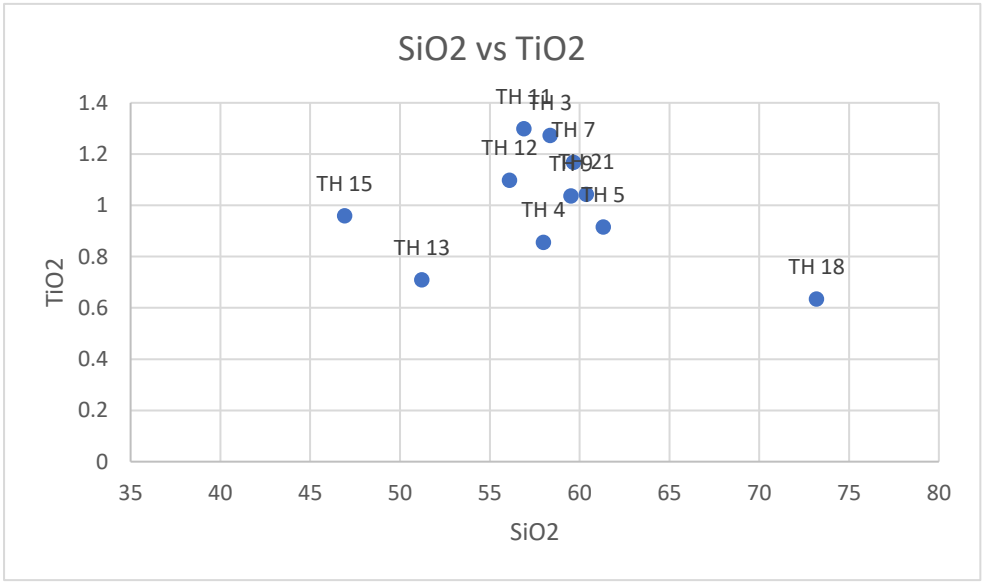


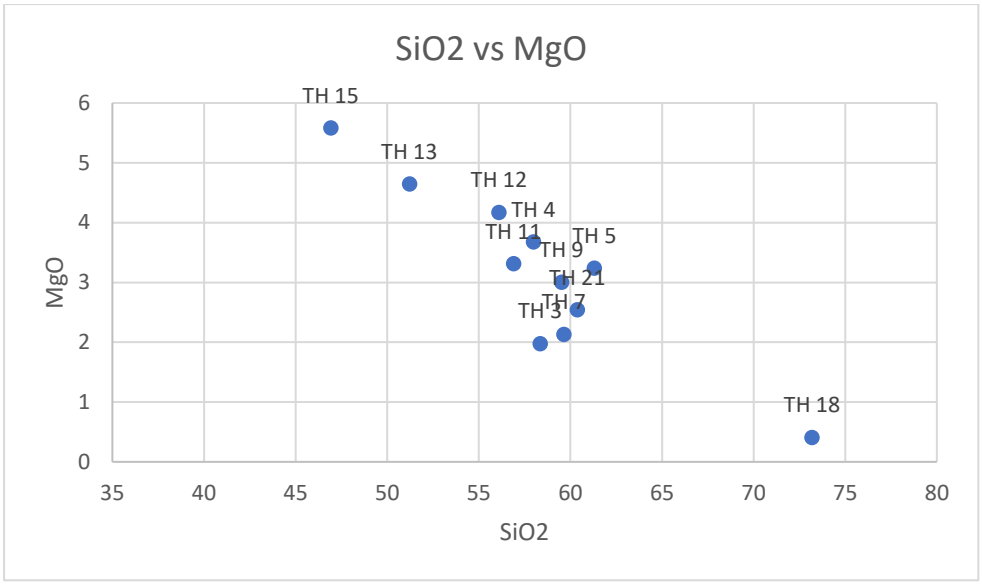
Figure 11: Total Alkali Silica diagram for samples from Thyolo Mountain

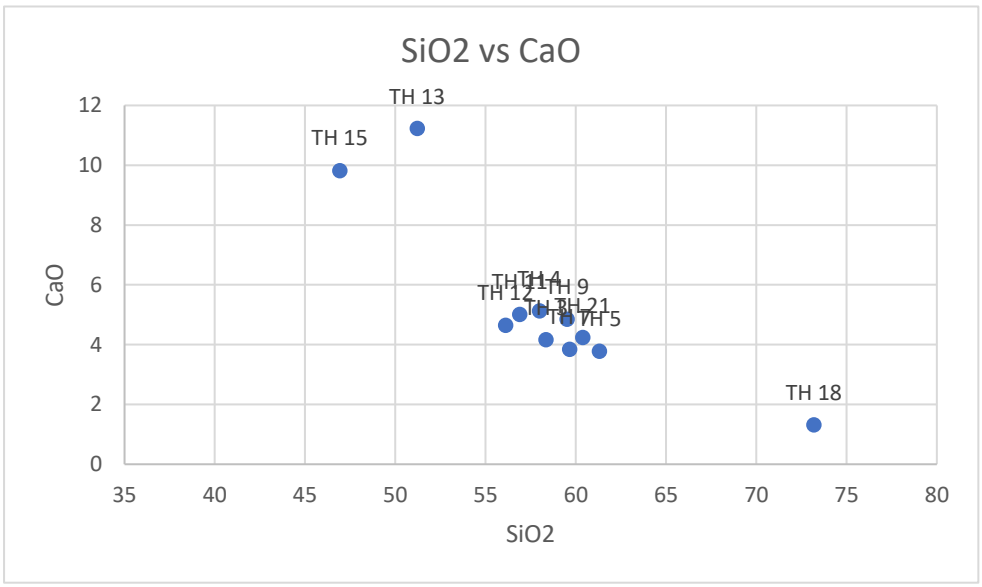
The SiO2 versus Fe2O3 plot shows a high composition of Fe2O3 in TH 15 and TH 13, suggesting a mafic to intermediate composition of these rocks. The lowest Fe2O3 values are observed in TH 18, typical of felsic rocks like granite. The SiO2 versus Al2O3 plot shows somewhat similar Al2O3 values across the samples with very small variations. The SiO2 versus CaO plot shows high values of CaO in TH 13 and TH 15, showing the mafic nature of the rocks. Low CaO values are observed in TH 18, which is typical of granites. SiO2 versus K2O plot shows high values of K2O in syenites like TH 3, TH9, etc, showing the presence of potassium-rich minerals or alkaline magmatism in continental rift zones. Low K2O values are observed in TH 15 and TH 13. Generally, low MnO values are observed in most of the samples, except TH 12, which looks like the odd one out of the bunch according to the SiO2 versus MnO plot. High TiO2 values are observed in syenite samples, and the lowest is observed in TH 18 according to the SiO2 versus TiO2 plot. High MgO is observed in TH 15 and TH 13, aligning them to the mafic part of the igneous rock spectrum. Somewhat intermediate values are observed in the syenite sample, with the lowest values observed in TH 18 according to the SiO2 versus MgO plot. High Na2O values are observed in syenite samples, aligning them with the felsic side of the igneous rock spectrum, suggesting explosive volcanism. Low values are observed in TH 15 and TH 13 according to the SiO2 against Na2O plot. P2O5 values are difficult to pinpoint with varying compositions across the board, with the lowest P2O5 values observed in TH 13 and TH 18.

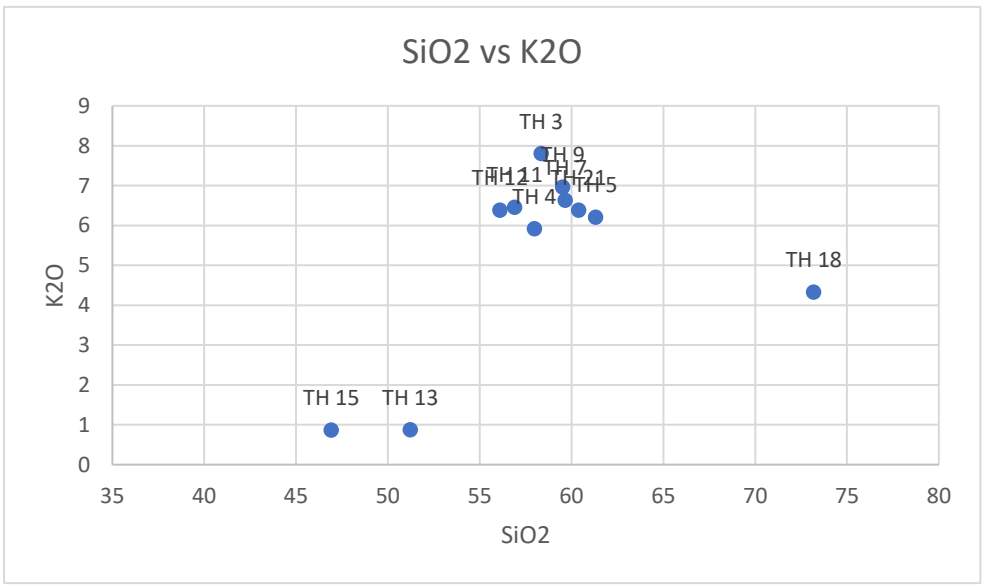

SiO2 vs Fe2O3
Fe2O3
SiO2
TH 15
TH 13
TH 18
TH 5
0
2
4
6
8
10
12
14
16
35
40
45
50
55
60
65
70
75
80

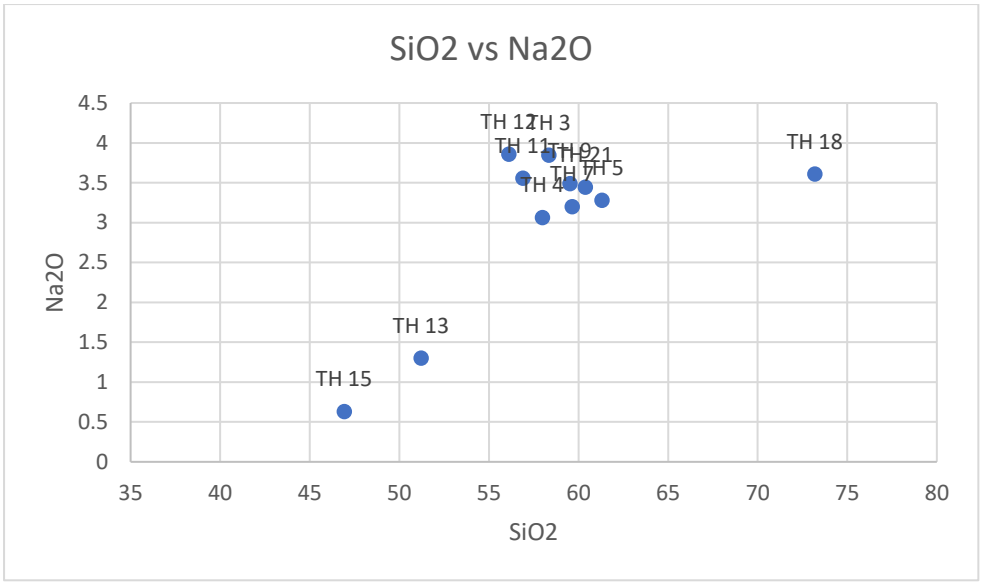

SiO2 vs Al2O3
Al2O3
SiO2
TH 15
TH 13
TH 18
0
5
10
15
20
25
35
40
45
50
55
60
65
70
75
80

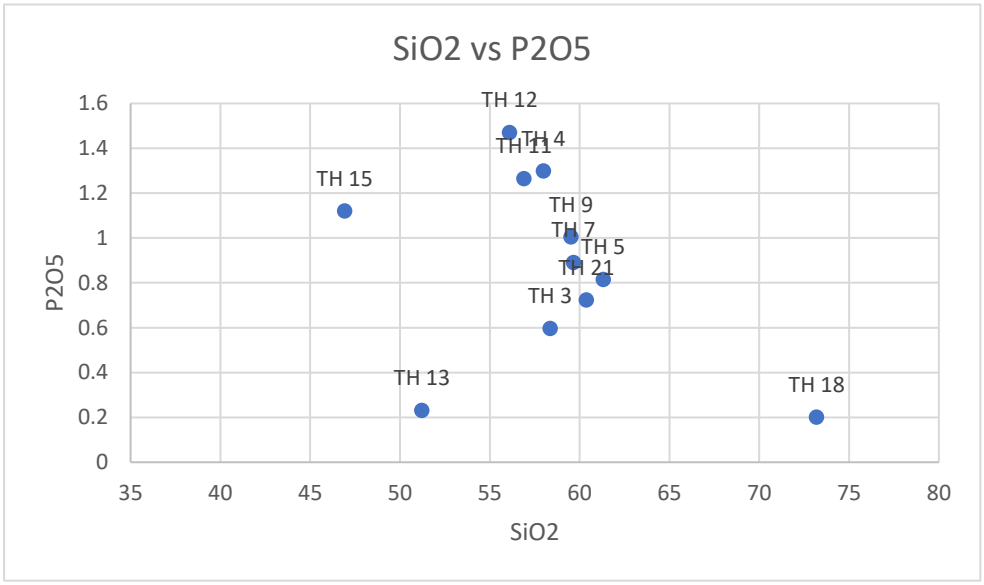

SiO2 vs TiO2
TiO2
SiO2
TH 15
TH 13
TH 12
TH 4
TH 5
TH 18
0
0.2
0.4
0.6
0.8
1
1.2
1.4
35
40
45
50
55
60
65
70
75
80


SiO2 vs MgO
TH 15
TH 13
TH 12
TH 4
TH 11
TH 5
TH 9
TH 21
TH 7
TH 3
TH 18
MgO
SiO2
0
1
2
3
4
5
6
35
40
45
50
55
60
65
70
75
80


SiO2 vs CaO
TH 13
TH 15
TH 18
CaO
SiO2
0
2
4
6
8
10
12
35
40
45
50
55
60
65
70
75
80


SiO2 vs K2O
TH 3
TH 9
TH 4
TH 18
TH 15
TH 13
K2O
SiO2
0
1
2
3
4
5
6
7
8
9
35
40
45
50
55
60
65
70
75
80





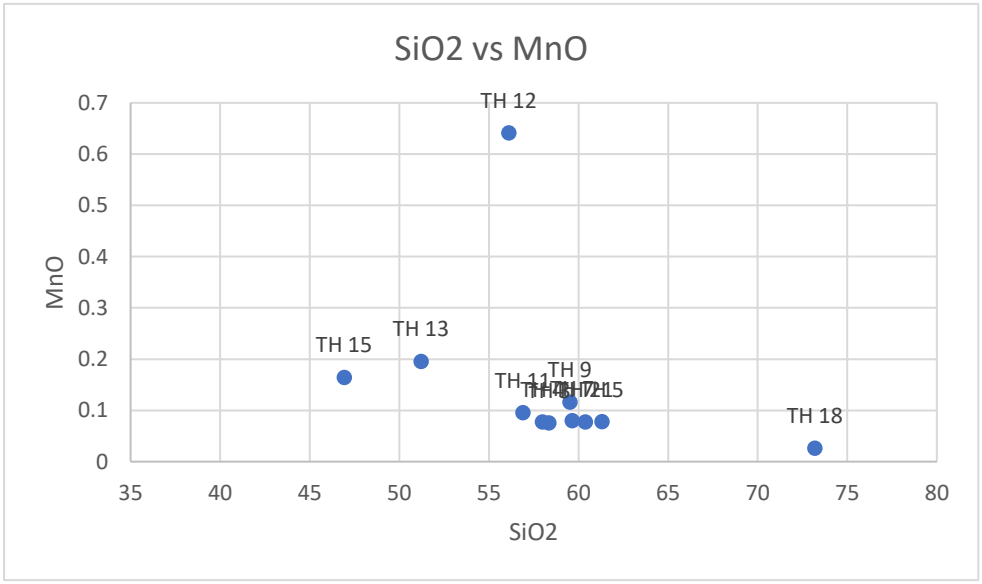


Figure 12: Major element versus SiO2 plots for samples from Thyolo Mountain

Trace element abundances in the samples vary across the board, with some significant and relatively high values observed. Some of the highest values of trace elements (in ppm) are observed in Ba (4593 - 354.5), Sr (2353 – 122.0), and Zr (413.5 – 83.9). The primitive mantle normalized trace elements data and the spider diagram show the enrichment of large ion lithophile elements (LILE) such as Rb, Ba, Th, etc. These elements are particularly concentrated in the late-stage products of magmatic crystallization (Misra, 2012). Primitive mantle normalized (McDonough & Sun, 1995) trace element data and spider diagram also show the depletion of high field strength elements like Nb, Zr, etc., relative to large ion lithophile elements. The patterns suggest late-stage magmatic crystallization

Table 4: Primitive Mantle-Normalized Trace Element Concentrations (ppm) for rock samples from Thyolo Mountain

normalized	Rb	Sr	Y	Zr	Nb	Ba	La	Ce	Nd	Pb	Th	Pr
TH 3	276.8333	66.63317	4.395349	48.90476	35.10638	356.8182	252.3148	142.8657	121.6	330.6667	96.85535	1.724138
TH4	148.8333	118.2412	3.930233	10.35238	8.81459	695.9091	201.5432	114.209	93.36	204	22.64151	108.2759
TH 5	237.1667	70.75377	4.465116	22.40952	23.1003	465.1515	231.9444	136.1194	99.6	321.3333	42.7673	97.58621
TH 7	280.5	85.8794	6.837209	44.5619	45.74468	523.3333	256.3272	164.6567	126.88	454	91.8239	111.3793
TH 9	236	90.25126	5.023256	41.54286	23.55623	478.3333	252.6235	143.8806	118	297.3333	69.18239	107.931

TH 11	250.3333	76.48241	6.790698	42.81905	41.18541	440.1515	266.358	166.3881	140.24	314	81.76101	138.6207
TH 12	206	90.40201	5.488372	8.333333	19.14894	555.1515	184.2593	107.0448	104.08	270	40.25157	80.68966
TH13	40.66667	7.100503	4.767442	8.866667	9.270517	53.71212	107.716	52.41791	43.28	10.66667	32.7044	130.6897
TH15	42.16667	6.130653	5.093023	7.990476	9.878419	61.95455	108.3333	49.31343	46.88	22	51.57233	136.2069
TH 18	145.6667	37.23618	0.139535	40.39048	20.06079	186.9697	160.4938	79.10448	64.72	241.3333	145.9119	109.3103
TH 21	255.5	74.47236	5.604651	28.29524	35.10638	403.3333	250.7716	157.791	128.96	317.3333	186.1635	144.4828

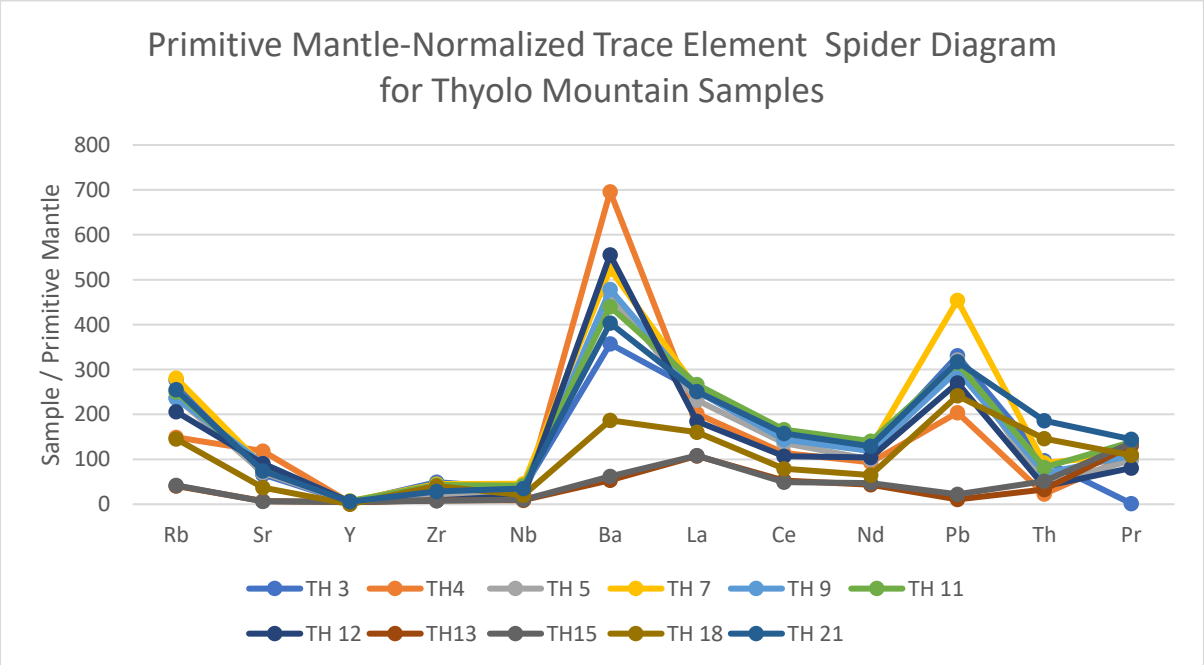


Figure 13: Primitive Mantle Normalized Spider Diagram for Samples from Thyolo Mountain

Chondrite-normalized (McDonough & Sun 1995) rare earth element (REE) patterns depicted by the spider diagram show enrichment patterns consistent with alkaline magmatism. Many of the samples are enriched in La, except for TH 13, TH 15, and TH 18. TH 13, TH 15, and TH 18 are depleted in most of the REEs except for Pr, which is depleted in the syenites and enriched in these samples. Most of the REEs are enriched in the syenites as observed in the spider diagram.

Table 5: Chondrite-Normalized Rare Earth Element (REE) Concentrations (ppm) for rock samples from Thyolo Mountain

Normalized(ppm)	La	Ce	Nd	Sm	Yb	Pr
TH 3	496.9605	276.6474	241.2698	9.359606	0.909091	5.208333
TH4	396.9605	221.1561	185.2381	3.694581	0.681818	327.0833
TH 5	456.8389	263.5838	197.619	3.694581	0.681818	294.7917
TH 7	504.8632	318.8439	251.746	3.694581	6.136364	336.4583
TH 9	497.5684	278.6127	234.127	3.694581	0.909091	326.0417
TH 11	524.6201	322.1965	278.254	5.172414	0.909091	418.75
TH 12	362.9179	207.2832	206.5079	3.694581	0.681818	243.75
TH13	212.1581	101.5029	85.87302	3.694581	7.727273	394.7917

TH15	213.3739	95.49133	93.01587	3.694581	8.409091	411.4583
TH 18	316.1094	153.1792	128.4127	3.694581	0.681818	330.2083
TH 21	493.921	305.5491	255.873	3.694581	0.681818	436.4583

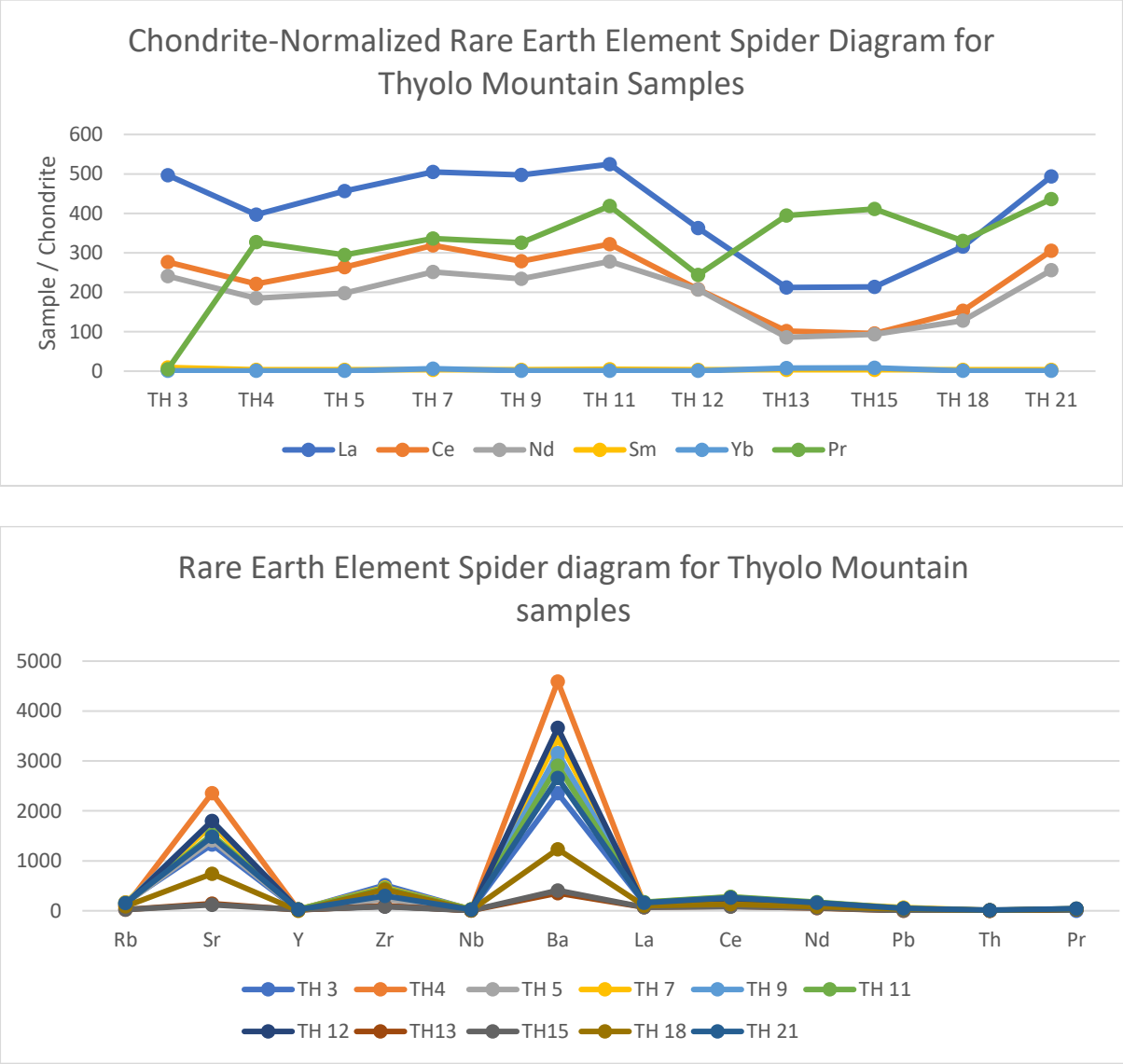


Figure 14: Chondrite-normalized Rare Earth Element (REE) Spider Diagram for samples from Thyolo Mountain *vs* Rare Element spider diagram for Thyolo Mountain samples

4.2. Alumina Saturation Indices (ASI)

Most of the samples are metaluminous, with TH 15 and TH 18 being slightly peraluminous, meaning they have slightly excess alumina relative to the major oxides, indicating different magma sources or differentiation processes. The peraluminosity plot helps classify the samples based on their aluminium content relative to the major element. The plot shows samples TH 15 and TH 18 as slightly peraluminous, while the rest are metaluminous, helping distinguish between peraluminous, metaluminous, and peralkaline rocks in the sample spectrum for Thyolo Mountain.

Table 6: Alumina saturation indices and classification

Sample ID	A/NK	A/CNK	Classification
TH 3	1.069602	0.707149	Metaluminous
TH 4	1.42654	0.785852	Metaluminous
TH 5	1.249762	0.797518	Metaluminous
TH 7	1.300936	0.833187	Metaluminous
TH 9	1.062936	0.638559	Metaluminous
TH 11	1.20346	0.703641	Metaluminous
TH 12	1.196831	0.731194	Metaluminous
TH 13	5.311709	0.697543	metaluminous (high A/NK)
TH 15	10.20105	1.018078	slightly peraluminous
TH 18	1.280341	1.045183	slightly peraluminous
TH 21	1.217152	0.754885	Metaluminous

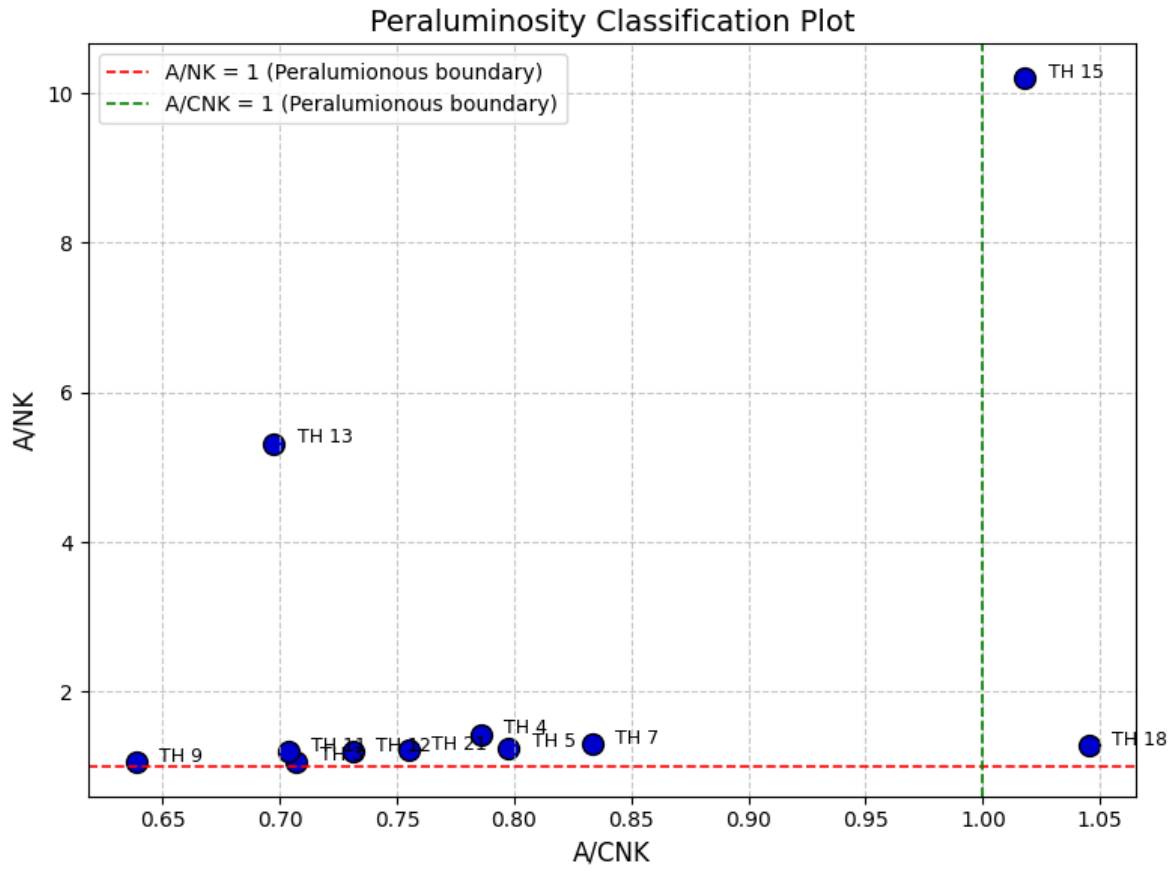
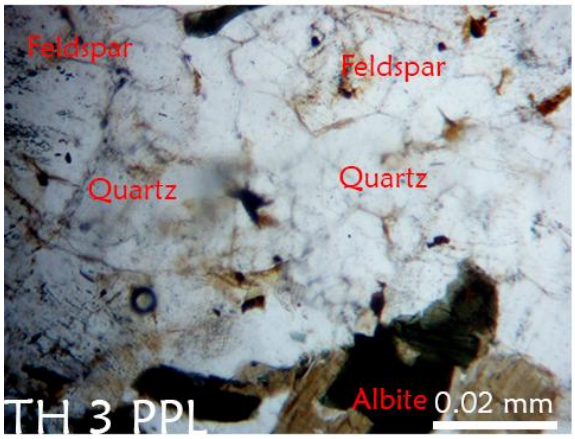
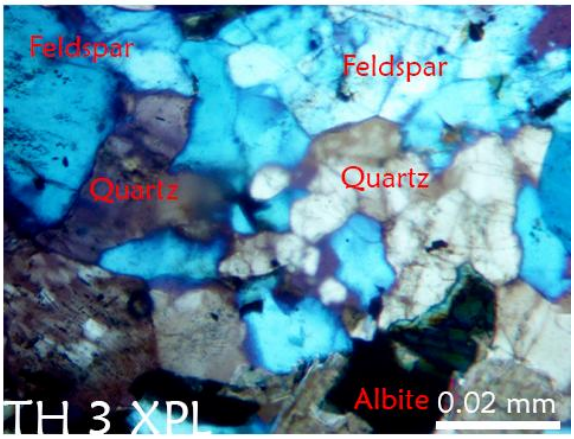


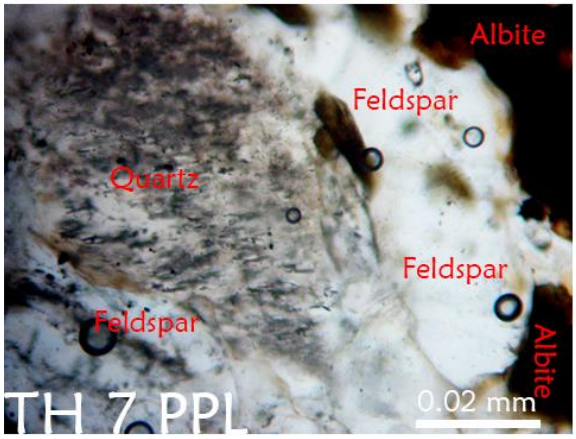
Figure 15: Peraluminosity Classification Plot for samples from Thyolo Mountain

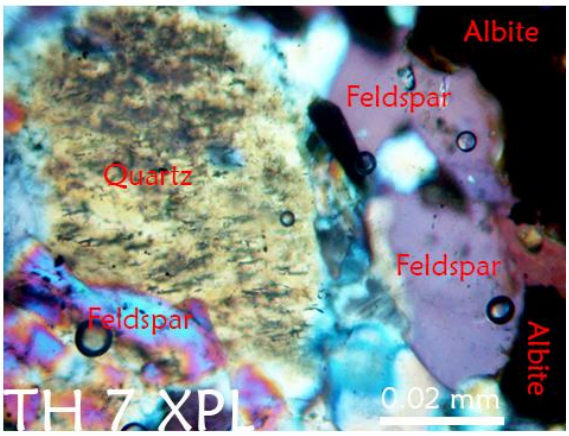
4.3. Petrographic Analysis

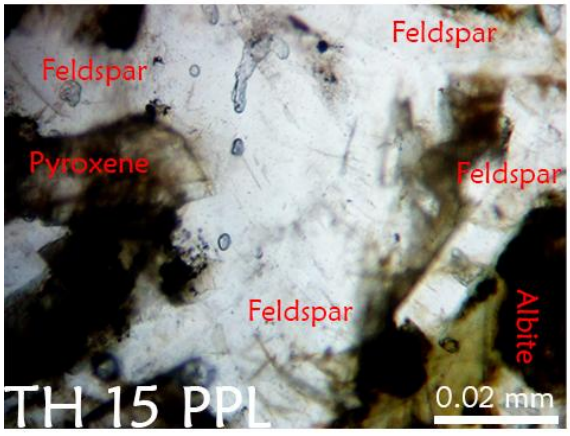
Thin-section microphotographs show the presence of feldspar minerals like orthoclase and anorthosite, which exhibit intertwined typical perthite texture. The microphotographs show granular texture with interlocking crystals typical of slowly cooling rocks formed deep in the crust. The microphotographs show perthitic textures like albite intergrowth in feldspar, they are special intergrowths of two types of feldspar. They depict deformation in sample TH 15, which suggests some tectonic processes that may be attributed to the East African Rift System. They show some form of alteration of in-sample TH 18, which may be attributed to metamorphic overprinting of the Thyolo mountain syenites or weathering. Feldspars are the predominant minerals in the samples according to the microphotographs, but various other minerals are present, like quartz, albite, pyroxene, etc.

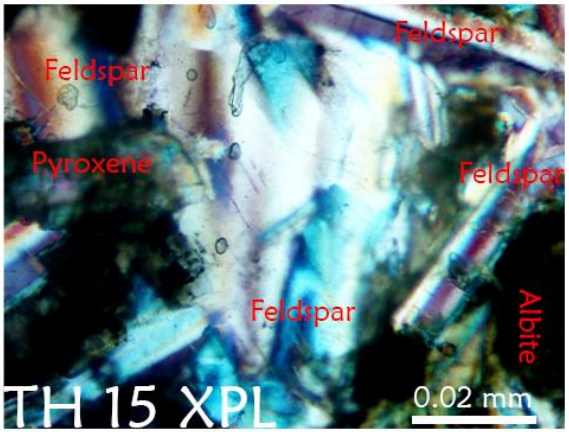

Feldspar
Feldspar
Quartz
Quartz
Albite
0.02 mm
TH 3 PPL


Feldspar
Feldspar
Quartz
Quartz
Albite
0.02 mm
TH 3 XPL


Albite
Feldspar
Quartz
Feldspar
Feldspar
Albite
0.02 mm
TH 7 PPL


Albite
Feldspar
Quartz
Feldspar
Feldspar
Albite
0.02 mm
TH 7 XPL


Feldspar
Feldspar
Pyroxene
Feldspar
Feldspar
Albite
0.02 mm
TH 15 PPL


Feldspar
Feldspar
Pyroxene
Feldspar
Feldspar
Albite
0.02 mm
TH 15 XPL

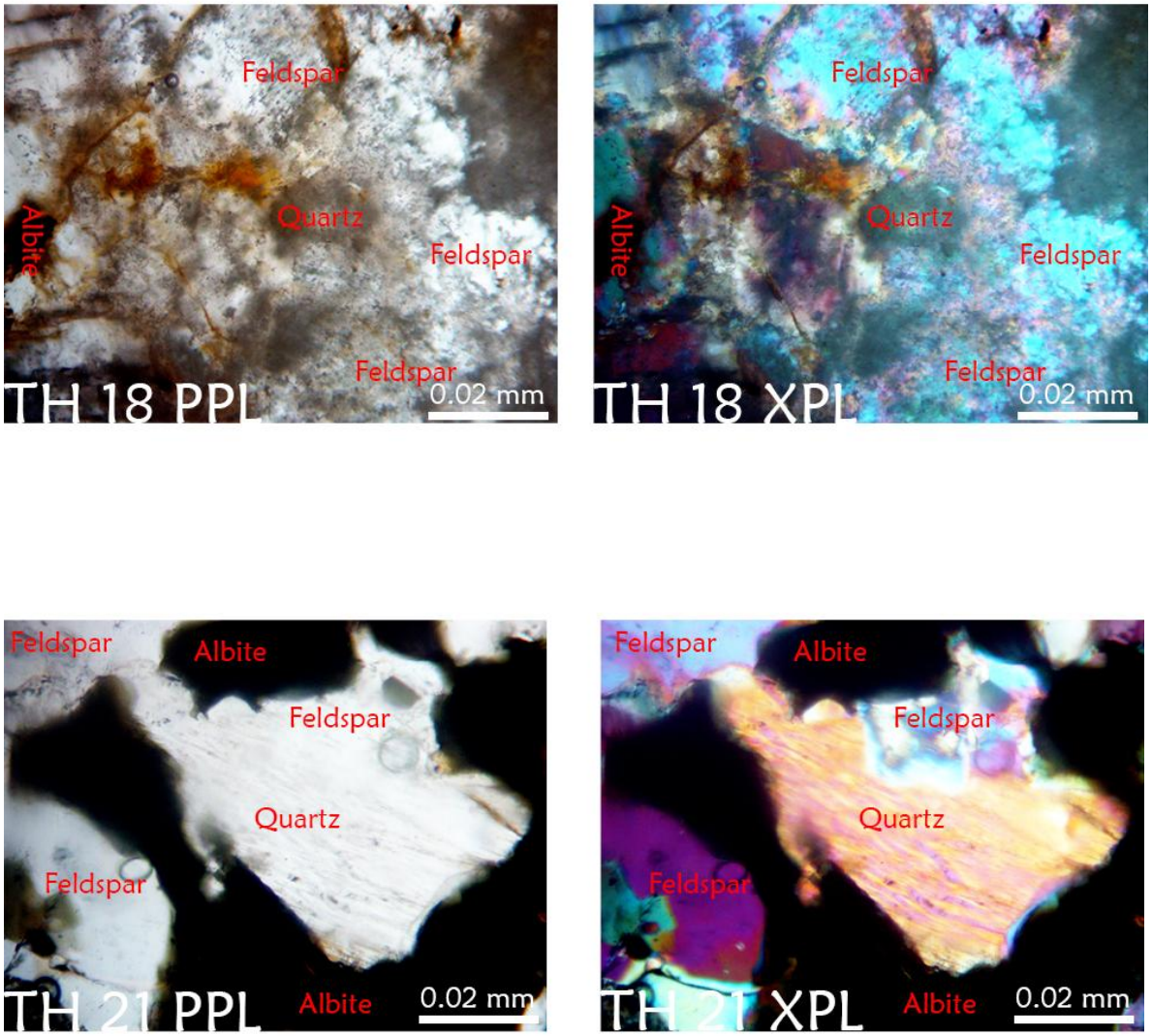


Figure 16: Microphotographs of Thyolo Mountain Samples

4.4. Statistical Analysis

4.4.1. Principal Component Analysis

PCA groups most of the syenite samples in the same region, proving their similar nature. PCA groups TH 13 and TH 15, revealing that they may have similar geochemical processes, such as alteration etc. TH 18 is isolated from most of the samples, proving its distinct nature and revealing that it is the outlier.

PCA biplot helps identify the elemental contributions to the principal components. For example, PR has a great influence on samples TH 13 and TH 15, while most of the trace

elements like La, Ce, Nd, etc. influence most of the syenite samples, as shown on the PCA biplot.

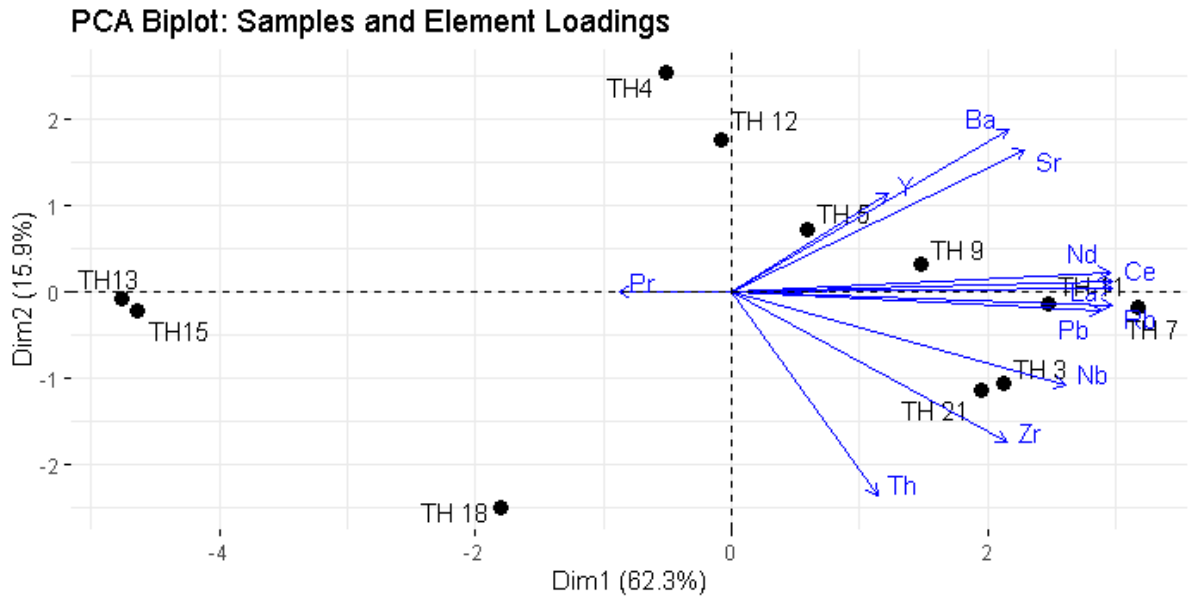


Figure 17: Principal Component Analysis Biplot of samples from Thyolo Mountain

4.4.2. Cluster Analysis

K-means groups the samples into two clusters. TH 13 and TH 15 belong to the same cluster, i.e., cluster 1, meaning they have similarities with reference to their trace element compositions. Most of the samples belong to cluster 0, as observed on the K-means clustering plot, which shows that syenite samples are similar in terms of trace element composition.

The silhouette plot quantifies the quality of the cluster analysis.

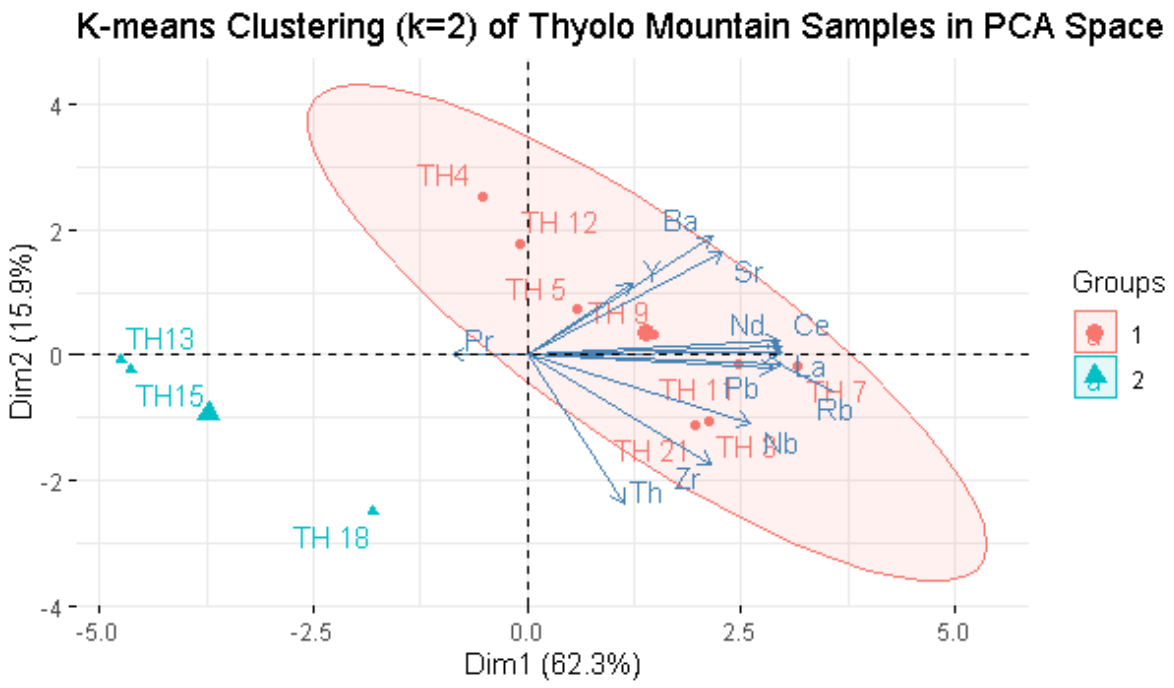


Figure 18: K-means Clustering in Principal Component Analysis Space of samples from Thyolo Mountain

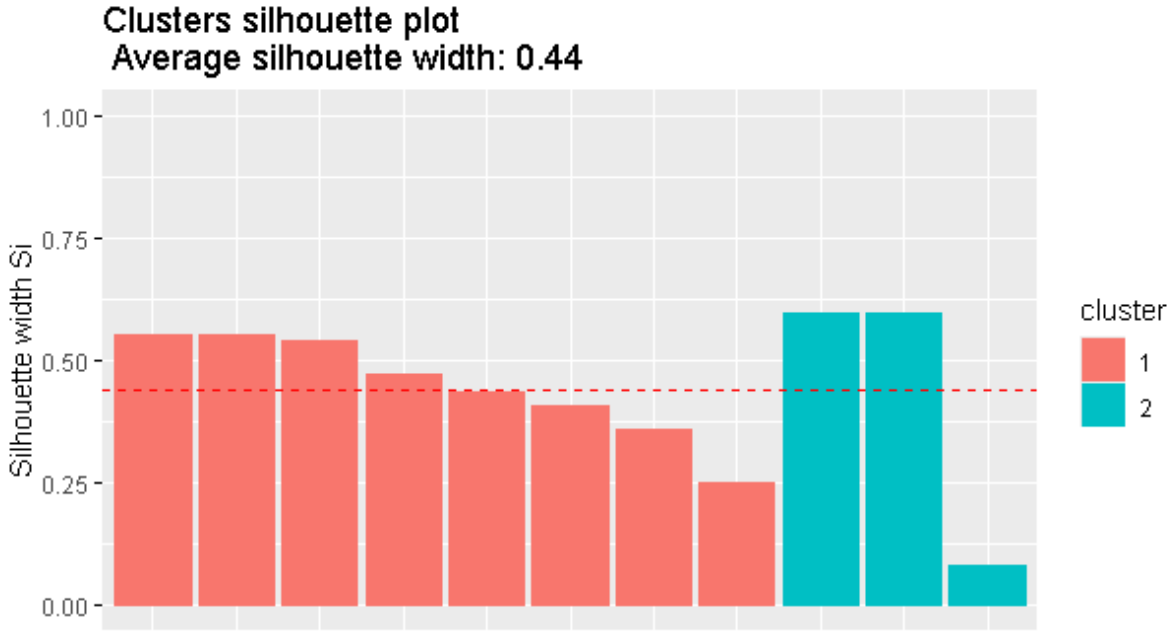


Figure 19: Silhouette Plot for K-means Clustering of samples from Thyolo Mountain

4.5. Discussions

Field, petrographic, geochemical, and statistical data were used to characterize each rock type, infer petrogenesis, evaluate tectonic context, and assess economic interest.

4.5.1. Characterization and Classification

The Thyolo mountain rocks are classified into three main rock types based on field observations, petrography, and geochemistry: perthitic syenites, granitic rocks, and perthite gneiss.

4.5.1.1. Syenitic Rocks

Syenitic rocks from the Thyolo mountain exhibit four colors: pink or brownish, dark grey, light grey, and whitish. Most of the rocks are phaneritic in texture, with a few porphyritic textures. The majority of the syenitic rocks show light and dark mineral grains, primarily alkali feldspars, oligoclase, hornblende, and minor quartz. These sections reveal granular textures and interlocking crystals indicative of slow cooling in a plutonic environment. Perthitic textures like albite lamellae in K-feldspar are prominent, confirming an alkaline nature.

Syenites have SiO2 contents ranging from 46.92 to 61.31 wt.% and average from 56 to 61 wt.%, typical of syenites (Le Maitre et al., 2002). High K2O (5.21 to 7.80 wt.%) and Na2O (2.70 to 3.85 wt.%) confirm the alkaline nature, plotting in the syenites or quartz syenite field on the total alkali silica (TAS) diagram. Most samples are metaluminous with high large ion lithophile elements (LILE) and depleted high field strength elements (HFSE). Chondrite-normalized REE patterns show LREE enrichment with no Eu, suggesting fractional crystallization of a differentiated magma.

These are metaluminous, alkaline syenites belonging to the shoshonite series, consistent with rift or post-orogenic magmatism (Kanouo et al., 2019)

4.5.1.2. Granitic rocks

They are represented by sample TH 18, the granitic rock is whitish, coarse-grained, with white and brownish mineral grains. Petrography shows perthitic feldspars, quartz, and minor mafic minerals. Alteration textures suggest weathering or metamorphic overprinting.

The 18 has high SiO2 73.19 wt.%, low Fe2O3 2.69 wt.%, and plots in the granite field on the TAS diagram. It is slightly peraluminous with lower LILEs compared to syenites. This suggests a more felsic, evolved magma.

TH 18 is a slightly peraluminous granite, likely an outlier due to its distinct composition, probably representing a late-stage differentiate or a separate intrusive phase.

4.5.1.3. Gneisses

They are represented by TH 13 and TH 15 are dark grey, coarse-grained, and dominated by dark mineral grains like hornblende and pyroxene. The petrography reveals perthitic feldspar, quartz, and mafic minerals, with deformation textures indicating tectonic influence likely linked to the East African Rift System (EARS) or earlier orogenic events, banding suggests high-grade metamorphism.

Gneiss has lower SiO2 39.39 to 44.38 wt.% and higher Fe2O3 11.42 to 13.75 wt.%.%, MgO 4.03 to 4.69 wt.% and CaO 8.24 to 9.73 wt.%, indicating a more mafic composition. They are metaluminous except TH15, which is slightly peraluminous. LILEs and REEs are depleted relative to syenites, but Pr is enriched, suggesting metamorphic recrystallization. PCA and K-means clustering group TH 13 and TH 15 together, distinct from syenites, due to their mafic trace element signatures

These are perthite gneisses, likely derived from a mafic intermediate protolith, metamorphosed under amphibolite to granulite facies conditions.

4.5.2. Petrogenesis

The petrogenetic processes responsible for the formation of the Thyolo mountains' syenites and gneisses are inferred from their geochemical and petrographic signatures.

4.5.2.1. Syenites

The alkaline nature, high K2O + Na2O > 9 wt.%, and LREE enrichment suggest derivation from a silica-oversaturated, alkali-rich magma. This is consistent with partial melting or lower crustal material in an extensional setting, possibly related to the EARS or post-orogenic events after the pan-African orogeny (Burke et al., 2003). But on the other hand they may also be due to low degree of partial melting associated with migmatization (Habgood et al., 1973). The metaluminous character indicated minimal

crustal contamination with magma differentiation driven by fractional crystallization of pyroxene, hornblende, and plagioclase.

Perthitic textures formed during slow cooling below the feldspar solvus (~700C °C), typical of deep crustal plutonic environments. The presence of porphyritic textures in some samples suggests multiple intrusive phases or variable cooling rates. The enrichment of LILE and depletion of HSFE in spider diagrams point to late-stage magmatic crystallization.

4.5.2.2. Granitic rocks

The high SiO2 values and peraluminous nature suggest derivation from partial melting of crustal material, possibly a late-stage magmatic event. The lower LILE and REE indicate a more evolved magma compared to the syenites.

The coarse-grained texture and alteration suggest slow cooling followed by weathering or low-grade metamorphism. TH 18 represents a differentiated fraction of the syenitic magma or a separate intrusive phase.

Similar granites occur in the CAP associated with late-stage felsic intrusions (Nyalugwe, 2019)

4.5.2.3. Perthite Gneisses

The mafic to intermediate composition and enrichment, likely a mafic intrusion or volcanic rock, metamorphosed under high-grade conditions, likely amphibolite to granulite facies. Deformation textures in TH 15 indicate tectonic force, possibly during the pan-African orogeny or EARS rifting.

Gneissic banding and perthitic textures suggest recrystallization during high-temperature metamorphism, with exsolution of albite in microcline occurring after metamorphism. The depletion of LILE relative to syenites may reflect element mobility during metamorphism.

Similar gneisses occur in the Mozambique belt, formed during Neoproterozoic-Cambrian collisions (Tsunogae et al., 2020).

4.5.3. Tectonic evolution

The tectonic setting of Thyolo Mountain's rocks is evaluated considering Malawi's position at the intersection of the Ubendian, Irumide, and Mozambique belts and its role in the EARS.

4.5.3.1. Syenites

The alkaline, shoshonitic nature and LREE enrichment suggest formation in an extensional or post-orogenic setting. Two possibilities are outlined below:

Neoproterozoic magmatism

The syenites may be likened to late pan-African extensional magmatism ~750 to 740 Ma, associated with alkaline trends along the Mozambique belt (Manjate, 2017). This lines up with Burke et al. (2003) hypothesis of alkaline magmatism marking pan-African suture zones, supporting Thyolo's role in Gondwana assembly

Mesozoic rifting

The syenites may also be related to Jurassic-Cretaceous rifting of the CAP, in sync with EARS initiation (Chiwona et al., 2020). Their association with the Thyolo fault scarp zone supports this, as faulting may have facilitated the rise of magma.

Geochemical similarities with CAP syenites favor a Mesozoic origin, but geochronological data are required to confirm their age.

4.5.3.2. Gneisses

The mafic composition and deformation textures suggest formation during high-grade metamorphism of the Mozambique belt, likely during the pan African orogeny ~800 to 550 Ma. The gneisses may represent metamorphosed mafic intrusions emplaced during earlier tectonic events like irumide orogeny or syn-orogenic magmatism. Deformation observed in TH 15 aligns with EARS-related faulting, indicating reactivation of basement structures (Wedmore et al., 2020).

Thyolo Mountain resides near the junction of the East African and Kuunga orogens, making it a key site for studying Gondwana assembly (Manda et al., 2018). The syenites and gneisses reflect a polyphase tectonic history, with Neoproterozoic collision and metamorphism overprinted by Mesozoic and Cenozoic rifting

4.5.4. Economic and industrial significance

the rocks of the Thyolo mountain have economic potential applications based on their mineralogy and geochemistry.

4.5.4.1. Perthitic syenites

The high feldspar content makes them suitable for ceramics, glass, and construction (Mouliom et al., 2022). Elevated Ba and Sr suggest potential for barite or strontiate deposits, though further exploration is needed. The absence of significant REE or base metal enrichment limits their ore potential compared to CAP carbonatites (Chiwona et al., 2020)

4.5.4.2. Perthite gneisses

Their durability and mafic mineral content make them suitable for construction aggregates, road base, or ornamental stone (Cavallo et al., 2022). Low trace element concentrations reduce their metallic mineral potential

4.5.4.3. Granitic rocks

The quartz and feldspar content supports use in ceramics or as dimension stone, but its isolated occurrence limits large-scale exploitation.

4.5.5. Environmental implications

The geochemical composition of these rocks influences their weathering products, affecting soil and water quality. High K2O and Na2O in syenites may contribute to alkaline soils, beneficial for agriculture but requiring management to prevent salinization. Low concentrations of toxic elements like As, Pb, etc. suggest minimal environmental risk, but weathering of mafic minerals in gneisses could release Fe or Mn, impacting water quality. These findings may inform environmental management in Thyolo's agricultural and water-sensitive areas (Rollinson & Pease, 2021).

Chapter 5 Conclusion and Recommendations

5.1. Conclusion

The study aimed to investigate the geochemical characteristics and petrography of perthitic syenites and perthite gneiss from Thyolo Mountain to understand their petrogenesis and history. Field observations, petrographic analysis, geochemical data, and statistical methods were used to characterize these rocks. The key findings are summarized as follows: Perthitic syenites: these rocks are predominantly pink or brownish, dark-grey, and whitish with phaneritic textures. They show high K2O and Na2O values, confirming their alkaline nature. Most of the samples are metaluminous, consistent with rift or post-orogenic magmatism. Granite: represented by sample TH 18, characterized by high SiO2 values and slightly peraluminous nature. There is a good chance it represents a late-stage differentiation or separate intrusive phase. Perthite gneiss: dark grey, coarse-grained, dominated by dark mineral grains like hornblende and pyroxene. They show mafic compositions and are distinct from syenites due to their trace element signatures. Perthitic syenites: derived from silica oversaturated, alkali-rich magma, indicative of extensional settings, possibly related to the East African Rift System (EARS) or post-orogenic events after the pan-African orogeny. Perthitic textures formed during slow cooling, typical of deep-seated crustal environments. Granite: high SiO2 values suggest derivation from partial melting of crustal material, maybe representing a differentiated fraction of the syenitic magma. Perthite gneisses: likely metamorphosed igneous protoliths under amphibolite and granulite facies conditions. Deformation textures indicate tectonic forces linked to either pan-African orogeny or rifting. The alkaline shoshonitic nature of the syenites suggests formation in an extensional or post-orogenic setting, potentially linked to Neoproterozoic magmatism or Mesozoic rifting associated with the Chilwa Alkaline Province (CAP). Gneisses reflect high-grade metamorphism within the Mozambique belt during the Pan-African orogeny, with deformation features aligning with EARS-related faulting. Perthitic syenites: suitable for ceramics, glass, and construction applications due to high feldspar content. Elevated Ba and Sr suggest potential for barite or strontiate deposits. Perthite gneisses: suitable for construction aggregates, road base, or ornamental stone due to their durability and mafic minerals. Granitic rocks: useful in ceramics or as dimension stone, but limited in large-scale exploitation due to isolated occurrence.

Geochemical composition influences weathering products, affecting soil and water quality. High K2O and Na2O in syenites may contribute significantly to agriculture, but require proper management to prevent salinization. Low toxic element concentrations suggest minimal environmental risk, though weathering could impact water quality.

5.2. Recommendations

Based on the findings of this investigation, the following recommendations are suggested:

Further geological investigations

Conduct geochronological studies to confirm the age of the Thyolo mountain rocks and better understand their tectonic evolution.

Perform mineralogical and further geochemical analyses to explore potential industrial applications and economic significance further.

Environmental management

Develop ways to manage alkaline soils derived from K2O and Na2O contents in syenites to optimize agricultural productivity while preventing salinization.

Community engagement

Engage local communities and stakeholders in geological surveys and resource management initiatives to ensure sustainable development and utilization of natural resources.

Promote programs to raise awareness about the geological significance and economic potential of the Thyolo mountain.

Resource development

Explore the economic potential identified, like barite and strontium, through targeted exploration.

Evaluate the potential of using Thyolo mountain rocks in local construction and industrial applications to support development.

Limitation

Limited sample size

Only 22 rock samples were collected from 20 outcrops on Thyolo Mountain. This relatively small sample size may not entirely represent the variability of rock types across the entire mountain.

Restricted analytical scope

While major, trace, and REEs were analyzed, other informative analyses, such as isotopic dating, were not available.

Lack of geochronological data limits the ability to constrain the timing of rock formation.

Sampling challenges

Some samples showed signs of weathering, which can complicate geochemical interpretations.

Difficulty in accessing certain areas of the mountain may have biased sampling locations.

Analytical limitations

Detection limits of XRF for some elements resulted in many “<” values

Chapter 6 References

References

Albarède, F. (2009). Geochemistry: An introduction (2nd ed.). Cambridge University Press.

Alexandre, P. (2021). Geochemistry: Pathways and processes. Columbia University Press.

Alling, H. L. (1937). The significance of perthite in igneous rocks. Journal of Geology, 45(6), 623–642. https://doi.org/10.1086/624567

Bai, X., Liu, S., & Wang, W. (2014). Zircon U-Pb-Hf isotopes and geochemistry of Neoarchean dioritic-trondhjemitic gneisses, Jiaodong terrane: Constraints on petrogenesis and tectonic setting. Precambrian Research, 247, 1–17. https://doi.org/10.1016/j.precamres.2014.03.007

Balaghi Einalou, M., Sadeghian, M., Ghasemi, H., & Mohajjel, M. (2014). Zircon U-Pb ages, Hf isotopes and geochemistry of the schists, gneisses and granites in the Delbar metamorphic-igneous complex, SE of Shahrood (Iran): Implications for the geologic history of the complex. Journal of Asian Earth Sciences, 94, 39 54. https://doi.org/10.1016/j.jseaes.2014.08.003

Bigot, L., & Jébrak, M. (2015). Gold mineralization in the Abitibi greenstone belt: The Young-Davidson syenite-hosted deposit, Matachewan, Ontario, Canada. Economic Geology, 110(6), 1499–1520. https://doi.org/10.2113/econgeo.110.6.1499

Bogva, J. (1950). Iron ore deposits in Greenland syenites. Geological Survey of Greenland Bulletin, 10, 1–25.

Bonewitz, R. L. (2012). Rocks and minerals. DK Publishing.

Bose, P. K. (1961). Perthosite and associated rocks in southern Malawi. Geological Magazine, 98(4), 321–328. https://doi.org/10.1017/S0016756800060123

Brooks, C. K. (1991). Nepheline sodalite syenites from the southern Blosseville coast, East Greenland. Journal of Petrology, 32(4), 767–790. https://doi.org/10.1093/petrology/32.4.767

Burke, K., Ashwal, L. D., & Webb, S. J. (2003). New way to map old sutures using deformed alkaline rocks and carbonatites. Geology, 31(5), 391–394. https://doi.org/10.1130/0091-7613(2003)031 <0391:NWTMOS>2.0.CO;2

Carter, G. S., & Bennett, J. D. (1973). The geology and mineral resources of Malawi. Geological Survey of Malawi.

Castaing, C. (1990). The lower Shire Valley: A reactivated segment of the East African Rift System. Journal of African Earth Sciences, 10(1–2), 111–122. https://doi.org/10.1016/0899-5362(90)90048-6

Cavallo, A., Bigi, S., & Di Luzio, E. (2022). Gneiss as a construction material: Applications in civil engineering. Bulletin of Engineering Geology and the Environment, 81(3), 112. https://doi.org/10.1007/s10064-022-02615-9

Chakraborti, T. M., Ray, A., & Deb, G. K. (2019). Mineralogy and geochemistry of gneisses from the Chotanagpur Granite Gneiss Complex, eastern India. Journal of Earth System Science, 128(4), 89. https://doi.org/10.1007/s12040-019-1118-7

Chapola, L. S., & Kaphwiyo, C. L. (1992). The Malawi Rift: Geology, tectonics, and seismicity. Tectonophysics, 209(1–4), 165–173. https://doi.org/10.1016/0040 1951(92)90015-8

Chisambi, J., Tsunogae, T., & Manda, B. (2022). Metamorphic evolution of the southern Malawi basement complex: Implications for supercontinent assembly. Precambrian Research, 371, 106582. https://doi.org/10.1016/j.precamres.2022.106582

Chisenga, C., Manda, B. W., & Chiwona, A. G. (2021). Geophysical and geochemical characterization of apatite mineralization in the Mlindi ring structure, southern Malawi. Journal of African Earth Sciences, 178, 104169. https://doi.org/10.1016/j.jafrearsci.2021.104169

Chiwona, A. G. (2020). Petrology and geochemistry of selected nepheline syenites from Malawi and their potential as alternative potash sources. Journal of African Earth Sciences, 162, 103689. https://doi.org/10.1016/j.jafrearsci.2019.103689

Chorowicz, J. (2005). The East African Rift System. Journal of African Earth Sciences, 43(1–3), 379–410. https://doi.org/10.1016/j.jafrearsci.2005.07.019

Dawai, D., Tchameni, R., & Bascou, J. (2022). The late Pan-African Guider syenite pluton, Cameroon: Petrology and geodynamic implications. Journal of African Earth Sciences, 186, 104426. https://doi.org/10.1016/j.jafrearsci.2021.104426

Deer, W. A., Howie, R. A., & Zussman, J. (2013). An introduction to the rock-forming minerals (3rd ed.). Mineralogical Society of Great Britain and Ireland.

Dowman, E., Harris, C., & Woolley, A. R. (2023). Nepheline syenites of the Chilwa Alkaline Province, Malawi: Petrology and geochemistry. Mineralogical Magazine, 87(2), 234–245. https://doi.org/10.1180/mgm.2022.123

El-Mezayen, A. M., Heikal, M. A., & Omar, S. A. (2015). Abu-Rusheid subsurface gneisses, southeastern Egypt: Mineralogical and geochemical characteristics. Arabian Journal of Geosciences, 8(11), 9513–9528. https://doi.org/10.1007/s12517-015-1906-2

Engvik, A. K., & Bingen, B. (2016). Mafic granulites and charnockitic gneisses in the early Paleozoic domains of northeastern Mozambique. Precambrian Research, 277, 208–226. https://doi.org/10.1016/j.precamres.2016.02.015

Engvik, A. K., Elvevold, S., & Jacobs, J. (2024). Cambrian orthopyroxene-bearing granitoids and gneisses in Dronning Maud Land, Antarctica: Implications for Pan-African orogeny. Precambrian Research, 400, 107245. https://doi.org/10.1016/j.precamres.2023.107245

Fazlnia, A. (2019). Sardasht syenite-monzonite-gabbro appinites intrusions, northwest Iran: Geochemical and petrological characteristics. Lithos, 344–345, 1–15. https://doi.org/10.1016/j.lithos.2019.06.014

Garson, M. S., & Walshaw, R. D. (1969). The geology of the Mulanje area, Malawi. Geological Survey of Malawi Bulletin, 21, 1–57.

Glass, J. J. (2013). Petrology: Principles and practice. Springer.

Gulson, B. L. (1972). Perthite granite and syenites from northern Sweden: Geochemical and isotopic characteristics. Contributions to Mineralogy and Petrology, 35(3), 199–212. https://doi.org/10.1007/BF00371203

Habgood, F., Garson, M. S., & Thatcher, E. C. (1973). The geology of the Thyolo area, Malawi. Geological Survey of Malawi Bulletin, 25, 1–68.

Haissen, F., Cambeses, A., & Montero, P. (2017). Kalsilite nepheline syenites of the Awsard intrusive massif, Reguibat Shield, West African Craton, Morocco. Journal of African Earth Sciences, 129, 1–15. https://doi.org/10.1016/j.jafrearsci.2016.12.014

Hall, A. (1987). Igneous petrology. Longman Scientific & Technical.

Hu, J., Liu, X., & Chen, L. (2014). Whole-rock major and trace element geochemistry of gneissic granites from the Jitang complex, Tibet. Lithos, 206–207, 148–162. https://doi.org/10.1016/j.lithos.2014.07.022

Huang, Y. (2017). Metamorphic and tectonic evolution of the southern Malawi basement complex: Implications for Gondwana amalgamation. Precambrian Research, 300, 287–302. https://doi.org/10.1016/j.precamres.2017.08.015

Hurai, V., Huraiová, M., & Konečný, P. (2010). Syenite petrogenesis in extensional tectonic settings. Geologica Carpathica, 61(5), 377–392. https://doi.org/10.2478/v10096-010-0023-3

Jacobs, J., Thomas, R. J., & Weber, K. (2005). The Chilwa Alkaline Province, Malawi: Geology and petrogenesis. Journal of African Earth Sciences, 42(1–5), 149–165. https://doi.org/10.1016/j.jafrearsci.2005.07.008

Jeremine, E. (1951). Baiebokoum perthite syenite and Passi perthite granulite, southern Chad. Bulletin de la Société Géologique de France, 1(6), 345–356.

Kanouo, N. S., Ekomane, E., & Yongue, R. F. (2019). Syenites as industrial minerals: Petrography and geochemistry. Journal of African Earth Sciences, 151, 1–12. https://doi.org/10.1016/j.jafrearsci.2018.11.013

Karmakar, S., & Schenk, V. (2016). Regional geology of Malawi: Mesoproterozoic orogenic rocks. Journal of Petrology, 57(7), 1395–1418. https://doi.org/10.1093/petrology/egw045

Klein, C., & Philpotts, A. R. (2013). Earth materials: Introduction to mineralogy and petrology. Cambridge University Press.

Lee, M. R., & Parsons, I. (1997). Perthite formation in alkali feldspars: Mechanisms and implications. American Mineralogist, 82(5–6), 557–570. https://doi.org/10.2138/am-1997-5-610

Le Maitre, R. W., Streckeisen, A., & Zanettin, B. (2002). Igneous rocks: A classification and glossary of terms (2nd ed.). Cambridge University Press.

Lewis, J. D., Eby, G. N., & Woolley, A. R. (2016). The Chilwa Alkaline Province: A review of its geology and mineralization. Mineralogical Magazine, 80(1), 1–22. https://doi.org/10.1180/minmag.2016.080.057

Liu, F., & Wei, C. (2020). Ultra-high temperature paragneisses from the Qian'an gneiss dome, East Hebei terrane, North China Craton. Journal of Metamorphic Geology, 38(4), 395–420. https://doi.org/10.1111/jmg.12524

Liu, S., & Xu, J. (2015). Gneissic structures and their tectonic significance. Geoscience Frontiers, 6(3), 335–344. https://doi.org/10.1016/j.gsf.2014.08.003

Lobach-Zhuchenko, S. B., Balagansky, V. V., & Baltybaev, S. K. (2017). Geochemistry and zircon geochronology of the Bug granulite-gneiss complex, Ukraine. Precambrian Research, 291, 150–172. https://doi.org/10.1016/j.precamres.2017.01.015

Luan, Y., Zhang, J., & Fan, J. (2019). Magmatic and metamorphic processes in the formation of syenitic and gneissic rocks. Geological Journal, 54(4), 2315–2327. https://doi.org/10.1002/gj.3303

Macgregor, D. S. (2015). History of the development of the East African Rift System: A series of interpreted maps through time. Journal of African Earth Sciences, 101, 232–252. https://doi.org/10.1016/j.jafrearsci.2014.09.016

Mahadevan, C., & Sathapathi, N. (1954). Syenites as building materials. Journal of the Geological Society of India, 1(1), 45–56.

Mahmoud, A. M. (2018). Syenites and granites of the El Garra Hamra complex, Egypt: Petrology and mineralization. Arabian Journal of Geosciences, 11(18), 567. https://doi.org/10.1007/s12517-018-3907-4

Malunga, G. W. P. (2018). Mineral resources of Malawi. Geological Survey of Malawi.

Manda, B. W., Cawood, P. A., & Spencer, C. J. (2018). The southern Malawi basement complex: Tectonic evolution and Gondwana assembly. Precambrian Research, 317, 147–163. https://doi.org/10.1016/j.precamres.2018.08.015

Manjate, C. F. (2017). Neoproterozoic alkaline magmatism in the Mozambique Belt: Implications for Gondwana assembly. Journal of African Earth Sciences, 133, 1 12. https://doi.org/10.1016/j.jafrearsci.2017.05.008

McDonough, W. F., & Sun, S.-s. (1995). The composition of the Earth. Chemical Geology, 120(3–4), 223–253. https://doi.org/10.1016/0009-2541(94)00140-4

Mikhailova, J. A., Pakhomovsky, Y. A., & Ivanyuk, G. Y. (2021). Poikilitic syenites of the Lovozero massif, Kola Peninsula, Russia. Mineralogy and Petrology, 115(2), 167–180. https://doi.org/10.1007/s00710-020-00729-9

Mishra, K. C. (2018). Gneiss formation and metamorphic processes. Journal of the Geological Society of India, 91(3), 321–329. https://doi.org/10.1007/s12594 018-0867-9

Misra, K. C. (2012). Introduction to geochemistry: Principles and applications. Wiley Blackwell.

Mouliom, A. M., Ndam, J. R., & Kouske, A. P. (2022). Petrography and geochemistry of the Ina syenite, central Cameroon: Implications for industrial applications.

Journal of African Earth Sciences, 188, 104471. https://doi.org/10.1016/j.jafrearsci.2022.104471

Mukherjee, S., Dey, A., & Ibanez-Mejia, M. (2017). Charnockitic gneisses of the Chotanagpur Granite Gneiss Complex, eastern India: Petrology and tectonic implications. Precambrian Research, 300, 151–172. https://doi.org/10.1016/j.precamres.2017.08.007

Mukherjee, S., Dey, A., & Sanyal, S. (2019). Bulk rock geochemistry of granitoids from the Chotanagpur Granite Gneiss Complex: Implications for petrogenesis. Lithos, 338–339, 1–15. https://doi.org/10.1016/j.lithos.2019.04.006

Nesse, W. D. (2000). Introduction to mineralogy. Oxford University Press.

Nyalugwe, V. (2019). Petrogenesis of syenites in the Chilwa Alkaline Province, Malawi. Journal of African Earth Sciences, 154, 1–10. https://doi.org/10.1016/j.jafrearsci.2019.03.008

Parsons, I. (1989). Syenites: Mineralogy and petrogenesis. Geological Society, London, Special Publications, 43(1), 329–339. https://doi.org/10.1144/GSL.SP.1989.043.01.25

Parsons, I. (2010). Feldspars and their reactions in igneous and metamorphic rocks. Mineralogical Magazine, 74(2), 193–221. https://doi.org/10.1180/minmag.2010.074.2.193

Petrella, L., Williams-Jones, A. E., & Goutier, J. (2014). Rare earth element mineralization in the Misy syenitic intrusion, northern Quebec, Canada. Economic Geology, 109(4), 1117–1132. https://doi.org/10.2113/econgeo.109.4.1117

Philpotts, A. R., & Ague, J. J. (2009). Principles of igneous and metamorphic petrology (2nd ed.). Cambridge University Press.

Piper, D. P., Garson, M. S., & Thatcher, E. C. (1989). Perthite augen gneisses in central Malawi. Geological Journal, 24(3), 191–204. https://doi.org/10.1002/gj.3350240303

Ramberg, I. B. (1972). Braid perthite and micro braid perthite from Permian nepheline syenite pegmatites in monzonite, Oslo graben, Norway. Norsk Geologisk Tidsskrift, 52(3), 241–254.

Ring, U. (1994). The influence of preexisting structure on the evolution of the Malawi Rift. Tectonics, 13(2), 313–326. https://doi.org/10.1029/93TC02888

Ring, U., Betzler, C., & Delvaux, D. (1997). Tectonic evolution of the East African region: Implications for Gondwana assembly. Geologische Rundschau, 86(2), 337–351. https://doi.org/10.1007/s005310050145

Rivett, M. O., Budimir, L., & Mannix, N. (2018). Geological controls on groundwater quality in Malawi. Environmental Earth Sciences, 77(14), 534. https://doi.org/10.1007/s12665-018-7710-7

Rollinson, H., & Pease, V. (2021). Using geochemistry to understand Earth's surface processes. Wiley-Blackwell.

Schønwandt, H. K., Borst, A. M., & Marks, M. A. W. (2023). Perthite in nepheline syenite from the Ilimaussaq complex, South Greenland. Mineralogical Magazine, 87(3), 389–402. https://doi.org/10.1180/mgm.2023.12

Scoon, R. N. (1958). The geology of the East African Rift System. Geological Magazine, 95(3), 193–205. https://doi.org/10.1017/S0016756800061153

Sedawie, T. (2023). Gemstones: Properties and applications. CSIRO Publishing.

Smedley, P. L., & Kinniburgh, D. G. (2013). A review of the source, behaviour and distribution of arsenic in natural waters. Applied Geochemistry, 18(6), 517 568. https://doi.org/10.1016/S0883-2927(02)00198-5

Sorensen, E. V., Kalvig, P., & Steenfelt, A. (2011). Uranium ore in agpaitic nepheline syenites, Greenland. Mineralium Deposita, 46(7), 711–727. https://doi.org/10.1007/s00126-011-0348-9

Sorokina, E. S., Nikandrov, S. N., & Kovalenko, V. I. (2017). Gem-quality corundum in syenites of the Ilmen Mountains, South Urals, Russia. Gems & Gemology, 53(2), 192–205. https://doi.org/10.5741/GEMS.53.2.192

Suhr, N., Hofmann, A., & Kröner, A. (2014). Granulite facies paragneisses of the Mahamba gneiss complex, central Swaziland. Precambrian Research, 247, 141 159. https://doi.org/10.1016/j.precamres.2014.03.015

Tsunogae, T., Yang, Q. Y., & Santosh, M. (2021). Metamorphic evolution of the southern Malawi basement complex: Implications for Gondwana amalgamation. Lithos, 394–395, 106168. https://doi.org/10.1016/j.lithos.2021.106168

Uher, P., Černý, P., & Chapman, R. (2006). Gem-quality corundum in syenites of the Cerova Mountains, Slovakia. The Canadian Mineralogist, 44(3), 645–657. https://doi.org/10.2113/gscanmin.44.3.645

Ugbe, F. C., Ogunleye, P. O., & Obadiah, O. (2023). Tectonic setting and geochemistry of syenites around Igarra, southwestern Nigeria. Journal of African Earth Sciences, 197, 104758. https://doi.org/10.1016/j.jafrearsci.2022.104758

Watkins, R. T., & Roex, A. P. (1991). Geochemistry of syenites: Implications for petrogenesis. South African Journal of Geology, 94(2–3), 145–156.

Wedmore, L. N. J., Biggs, J., & Floyd, J. (2020). Geodetic constraints on the Thyolo fault, southern Malawi: Implications for the East African Rift System. Geophysical Journal International, 222(3), 1957–1971. https://doi.org/10.1093/gji/ggaa283

Winter, J. D. (2001). An introduction to igneous and metamorphic petrology. Prentice Hall.

Wu, M., Zhao, G., & Sun, M. (2014). Geochemistry and Sm-Nd isotopes of Archean granitoid gneisses in the Jiaodong terrane: Constraints on petrogenesis and tectonic setting. Precambrian Research, 243, 1–16. https://doi.org/10.1016/j.precamres.2013.12.013

Xiao, W. (2005). Syenite petrogenesis in extensional settings: A global perspective. Earth-Science Reviews, 71(3–4), 175–199. https://doi.org/10.1016/j.earscirev.2005.04.002

Xu, C., Campbell, I. H., & Kynicky, J. (2004). Rare earth element geochemistry of the Maoniuping carbonatite-syenite complex, Sichuan Province, China. Economic Geology, 99(7), 1507–1526. https://doi.org/10.2113/gsecongeo.99.7.1507

Zhang, J., Linnen, R. L., & Lin, S. (2014). Gold mineralization in the Young-Davidson syenite-hosted deposit, Matachewan, Ontario. Economic Geology, 109(4), 1071–1088. https://doi.org/10.2113/econgeo.109.4.1071